



**HAL**  
open science

## Membrane lipid composition of *Carnobacterium maltaromaticum* CNCM I-3298, a highly cryoresistant lactic bacterium

Ha Phuong Ta, C. Clarisse, E. Maes, N. Yamakawa, Y. Guérardel, F. Krzewinski, W. Zarzycka, D. Touboul, Amélie Girardeau, Fernanda Fonseca, et al.

### ► To cite this version:

Ha Phuong Ta, C. Clarisse, E. Maes, N. Yamakawa, Y. Guérardel, et al.. Membrane lipid composition of *Carnobacterium maltaromaticum* CNCM I-3298, a highly cryoresistant lactic bacterium. *Chemistry and Physics of Lipids*, 2023, 255, pp.105326. 10.1016/j.chemphyslip.2023.105326 . hal-04397076

**HAL Id: hal-04397076**

**<https://hal.science/hal-04397076v1>**

Submitted on 16 Jan 2024

**HAL** is a multi-disciplinary open access archive for the deposit and dissemination of scientific research documents, whether they are published or not. The documents may come from teaching and research institutions in France or abroad, or from public or private research centers.

L'archive ouverte pluridisciplinaire **HAL**, est destinée au dépôt et à la diffusion de documents scientifiques de niveau recherche, publiés ou non, émanant des établissements d'enseignement et de recherche français ou étrangers, des laboratoires publics ou privés.

## Membrane lipid composition of *Carnobacterium maltaromaticum* CNCM I-3298, a highly cryoresistant lactic bacterium

HP. Ta<sup>1,\*</sup>, C. Clarisse<sup>2</sup>, E. Maes<sup>2</sup>, N. Yamakawa<sup>2</sup>, Y. Guérardel<sup>3,4</sup>, F. Krzewinski<sup>3</sup>, W. Zarzycka<sup>5</sup>, D. Touboul<sup>5</sup>, A. Girardeau<sup>6</sup>, F. Fonseca<sup>6</sup>, A. Kermarrec<sup>1</sup>, M. Viau<sup>1</sup>, A. Riaublanc<sup>1</sup>, MH. Ropers<sup>1</sup>

<sup>1</sup>: INRAE, BIA, F-44316, Nantes, France

<sup>2</sup>: Univ. Lille, CNRS, INSERM, CHU Lille, Institut Pasteur de Lille, US 41-UAR 2014-PLBS, F-59000 Lille, France

<sup>3</sup>: Univ. Lille, CNRS, UMR 8576 - UGSF - Unité de Glycobiologie Structurale et Fonctionnelle, F-59000 Lille, France

<sup>4</sup>: Institute for Glyco-core Research (iGCORE), Gifu University, Gifu, Japan

<sup>5</sup>: Université Paris-Saclay, CNRS, Institut de Chimie des Substances Naturelles, UPR 2301, 91198, Gif-sur-Yvette, France.

<sup>6</sup>: Université Paris-Saclay, INRAE, AgroParisTech, UMR SayFood, F-91120 Palaiseau, France

\*: [corresponding author, haphuong.ta@inrae.fr](mailto:haphuong.ta@inrae.fr)

Citation: Ta, H.P.; Clarisse, C.; Maes, E.; Yamakawa, N.; Guérardel, Y.; Krzewinski, F.; Zarzycka, W.; Touboul, D.; Girardeau, A.; Fonseca, F.; et al. Membrane lipid composition of *Carnobacterium maltaromaticum* CNCM I-3298, a highly cryoresistant lactic bacterium. *Chem. Phys. Lipids* 2023, 255, 105326 (<https://doi.org/10.1016/j.chemphyslip.2023.105326>)

## Abstract

The growing consumption of fermented products has led to an increasing demand for lactic acid bacteria (LAB), especially for LAB tolerant to freezing/thawing conditions. *Carnobacterium maltaromaticum* is a psychrotrophic and freeze-thawing resistant lactic acid bacterium. The membrane is the primary site of damage during the cryo-preservation process and requires modulation to improve cryoresistance. However, knowledge about the membrane structure of this LAB genus is limited. We presented here the first study of the membrane lipid composition of *C. maltaromaticum* CNCM I-3298 including the polar heads and the fatty acid compositions of each lipid family (neutral lipids, glycolipids, phospholipids). The strain CNCM I-3298 is principally composed of glycolipids (32%) and phospholipids (55%). About 95% of glycolipids are dihexaoyldiglyceride while less than 5% are monohexaoyldiglyceride. The disaccharide chain of dihexaoyldiglyceride is composed of  $\alpha$ -Gal(1-2)- $\alpha$ -Glc chain, evidenced for the first time in a LAB strain other than lactobacillus strains. Phosphatidylglycerol is the main phospholipid (94%). All polar lipids are exceptionally rich in C18:1 (from 70 to 80%). Regarding the fatty acid composition, *C. maltaromaticum* CNCM I-3298 is an atypical bacterium within the genus *Carnobacterium* due to its high C18:1 proportion but resemble the other *Carnobacterium* strains as they mostly do not contain cyclic fatty acids.

### Highlights:

- Membrane lipids of *C. maltaromaticum* CNCM I-3298 is principally composed of glycolipids (32%) and phospholipids (55%).
- All polar lipids are exceptionally rich in C18:1 (from 70 to 80%)
- About 95% of glycolipids are dihexaoyldiglycerides. Less than 5% are monohexaoyldiglycerides.
- The disaccharide chain of dihexaoyldiglycerides is composed of  $\alpha$ -Gal(1-2)- $\alpha$ -Glc chain.
- Phosphatidylglycerol is the principal phospholipid (94%).

### Keywords

Lactic acid bacteria; *Carnobacterium maltaromaticum*; glycolipid; phospholipid; mass spectrometry; NMR

## Introduction

Lactic acid bacteria are widely used in the fermentation of foods such as meat, vegetables, fruits and dairy products. This process helps to increase the storage time of foods and at the same time confers various interesting organoleptic properties to the aliments, for example flavors or texture (1,2). Today, their utilization has been reinforced by the urge for natural, healthy and even functional foods due to the increasing demands of consumers (1,2).

The commercialization of these bacteria requires appropriate conservation conditions in order to preserve their viability and functionality (3). Processes such as freezing and freeze-drying have commonly been used for preserving these industrial starters (4). However, the viability and the acidification activity of the concerned strains might be significantly altered during the preservation processes (3,5) reducing their efficiency and causing economic losses. Different approaches have been used to reduce these negative effects, such as: modification of the culture conditions to make more resistant strains, optimization of the freezing process and utilization of cryo-protectants (6–8).

The primary site of damage following the freezing of bacteria is the cellular membrane (9,10). To understand the cryo-preservation of the lactic acid bacteria, researchers' investigations have focused on the membrane lipid composition of these bacteria. However, reported studies have paid attention almost exclusively to the fatty acid properties such as the concentration of unsaturated fatty acids and the significant presence of the cyclopropane containing fatty acids (9,11–13). One explanation proposed for the role of such fatty acid chains in freeze-thaw resistance was that they provide a certain fluidity to the cellular membrane and consequently, increase their cellular membrane flexibility to adapt to the changes of the exterior environment (9,14). In fact, both the fatty acid composition and the polar head lipid compositions are actors for the membrane structure and fluidity (11,15–18). Moreover, the glycolipids, which were identified in many LAB membranes (19–21), could form more orderly rigid structures within membranes alone as well as in various combinations with phospholipids (17). Such reported properties showed the need for a complete characterization of the membrane lipid structure for the understanding of bacterial cryoresistance. Yet, to our knowledge, the polar head lipid composition and the fatty acid composition of each lipid family of LAB have rarely been studied simultaneously. This is the objective of the present study.

We considered *C. maltaromaticum*, formerly *C. piscicola* (22), a psychrotrophic, gram-positive rod-shaped LAB (23) which are highly tolerant to freezing/thawing and high pressure (24–26). *C. maltaromaticum* strains are widely found in natural environments and especially in various ranges of food products including meat, fish, shrimp and dairy products (24,27). Scientific investigations have emphasized their organoleptic and technological effects in different kinds of foods (24,28–31). They have been used commercially to inhibit food-borne pathogens including *Listeria spp.* and *Pseudomonas spp.* (28,31–33). We focused our

work on the strain *C. maltaromaticum* CNCM I-3298 which has been used in Time-Temperature Integrators (TTI) for food applications (34–36). This strain exhibits no loss of viability or acidification activity even after several freeze-thawing cycles, regardless of applied culture conditions (temperature and pH) (37). Since the lipids of gram-positive bacteria are found essentially in the cellular membrane (38,39), we extracted the whole cellular lipids in order to study the membrane lipid composition of *C. maltaromaticum* CNCM I-3298 and discuss its properties in comparison to other LAB.

## Materials and Methods

### Reagents and chemicals

Sodium chloride (purity 100%) was purchased from NormaPur (VWR International S.A.S, France). Sodium hydroxide was from VWR (Radnor, PA 19087, United States). Alpha – naphthol and primuline (both of 99%), trimethylsulfonium hydroxide (TMSH, ~ 0.25 M in methanol, LiChropur quality), anhydrous methanol, acetyl chloride, silver carbonate, heptane, bis-silyltrifluoroacetamide (BSTFA), pyridine, 2,5-dihydroxy benzoic acid (DHB), boron trifluoride-methanol solution (14% in methanol) and additive for ESI-MS analysis like ammonium acetate (LC-MS grade) were from Sigma-Aldrich (Saint-Quentin Fallavier, France). Ninhydrin (99%) was from Merck (Darmstadt, Germany).

Solvents were chloroform (stabilized with ethanol), acetone and methanol (all of 99.9% purity and HPLC grade), cyclohexane (99.8%, HPLC grade), 30% ammonia solution for analysis, toluene for analysis, absolute ethanol (99.9%), ethanol (HPLC grade) from Carlo Erba Reagents (Val de Reuil, France) and butanol (99.4%) from Sigma-Aldrich (Saint-Quentin Fallavier, France). Specifically, methanol (HPLC grade) for ESI-MS analysis was purchased from J.T. Baker (Center Valley, PA, USA). Carbon dioxide (purity 99.7% or greater) was purchased from Air Liquide (Grigny, France). Water was of ultrapure quality (MilliQ Reference A+, 18.2 M $\Omega$ .cm at about 20°C).

Nonanoic acid (C9:0, 99%), cis-11,12-methyleneoctadecanoic acid (lactobacillic acid, cycC19:0, 99%) were from LGC Standards (Molsheim, France). Oleic acid (99% purity) and neutral lipid standard mixture, (monoolein, 1,2 and 1,3 dioleoyl-glycerol and trioleoyl glycerol) were purchased from Sigma Aldrich. 1,2-Dimyristoyl-*sn*-glycero-3-phosphoethanolamine (DMPE), 1,2-Dioleoyl-*sn*-glycero-3-phospho-L-serine (DOPS), 1,2-Dioleoyl-*sn*-glycero-3-phospho-(1'-*rac*-glycerol) (DOPG), 1-Palmitoyl-2-Oleoyl-*sn*-Glycero-3-Phosphatidylglycerol (POPG), L- $\alpha$ -lysophosphatidylethanolamine (LysoPE, Egg, Chicken), 1,2-diacyl-3-O-( $\alpha$ -D-galactosyl 1-6)- $\alpha$ -D-galactosyl-*sn*-glycerol (Digalactosyldiacylglycerol, DGDG), 1,2-diacyl-3-O- $\beta$ -D-galactosyl-*sn*-glycerol (Monogalactosyldiacylglycerol, MGDG), LightSPLASH (phospholipids) and other phospholipid standards all of at least 99% purity were purchased either directly from Avanti Polar Lipids (Alabaster, Alabama, USA) or through Sigma Aldrich (Saint Quentin Fallavier, France). Methyl fatty

acid standard (Supelco 37 component fatty acid methyl esters FAME mix) was purchased from Sigma-Aldrich (Saint-Quentin Fallavier, France).

### **Cultivation of *C. maltaromaticum* CNCM I-3298**

*C. maltaromaticum* CNCM I-3298 was produced under industrial production conditions, *i.e.* pH 7, 30°C and a harvest time close to the beginning of the stationary phase (37). Stock culture in milk supplemented with 15% (w/w) of glycerol was stored at -80°C. 100 µL of stock culture was first incubated for 13-16 hours at 30°C in 10 mL of sterilized medium (referred to as MN medium) composed of the following ingredients: trehalose, proteose peptone, yeast extract, Tween 80, MnSO<sub>4</sub>, and MgSO<sub>4</sub> as detailed by Girardeau *et al.* (37). Then 1 mL of this suspension was added to 50 mL of sterilized MN medium for another incubation at 30°C for 11 hours. The fermentation in the 3.5 L bioreactor was initiated at 107 CFU approximately, in sterilized MN medium (pre-adjusted to pH 7), at 30°C under agitation (150 rpm). The pH of the culture was automatically adjusted during the fermentation by the addition of 5 N sodium hydroxide. Cells were harvested one hour after the end of the exponential phase was reached. The cell suspensions were then cooled down at 4°C in an ice-water bath and concentrated by centrifugation (2635 g for 10 min at 4°C). The cellular pellets obtained were resuspended at 4°C in the sterile protective medium (20% trehalose and 0.89% sodium chloride) at a ratio of 1:2 (w/w). The protected bacterial suspension was frozen at -80°C before being transported in dry ice then stored at -80°C until use.

### **Lipid extraction and isolation**

#### **Total lipid extraction**

The total membrane lipids of *C. maltaromaticum* were extracted following the Bligh-Dyer method (40). *C. maltaromaticum* cell suspension in the protective medium composed of 20% (w/w) trehalose in saline solution (8.9 g of NaCl/L) was kept frozen at -80°C. Just before use, the cell suspension was completely thawed out gradually in the fridge to avoid causing any stress that could modify the lipid composition of the bacteria (41). In order to limit the modification of membrane lipids during the extraction, lipids were extracted directly from the wet cells without drying step (41).

For each extraction, 10 mL of cell suspension was transferred to a 50 mL falcon tube. After centrifugation (5000 rpm, 4°C, 30 min) the supernatant was removed and the residue was washed twice with 10 mL of 0.89% sodium chloride solution.

The wet cell pellet was transferred to a 50 mL glass tube with 3.2 mL of water and then 21.6 mL of chloroform-methanol (1:2, v/v) was added. The suspension was shaken at 150 rpm at room temperature (RT, ~20°C) with intermittent vortexing for three hours. After centrifugation (2000 rpm, 20°C, 15 min), the supernatant was transferred to another 50 mL glass tube. Then 14.4 mL of water and 14.4 mL of chloroform

were added to this solution. The lower phase containing the total lipid extract was collected after centrifugation (2000 rpm, 20°C, 15 min). The organic solvent was removed first under vacuum using a rotary evaporator at 35°C and subsequently, under a nitrogen flow. The obtained residue was weighed and then was diluted in 1 mL of chloroform before being fractionated on a silica solid phase extraction (SPE) cartridge.

#### **Lipid class separation by solid phase extraction**

The total lipid extract was fractionated into neutral lipids, glycolipids and phospholipids on a silica SPE column (41) (SEP-PAK silica classic cartridges, Waters). A total extract of about 30 mg of lipids in chloroform was loaded to a SEP-PAK silica classic cartridge (previously conditioned with methanol then washed with chloroform). The neutral lipid fraction was eluted with 20 mL of chloroform (chloroform fraction). Two glycolipid fractions were obtained successively with 20 mL of chloroform – acetone (50:50, v/v) (chloroform-acetone fraction) and 20 mL acetone (acetone fraction). The phospholipid fraction was finally eluted with 20 mL of methanol (methanol fraction). Solvents were eliminated from all fractions under vacuum at 35°C using a rotary evaporator and then under a nitrogen flow. The weighed residues were diluted in either chloroform or chloroform: methanol (1:3, v/v) to a concentration of 2 to 4 mg/mL then stored at -20°C until use.

#### **Thin Layer Chromatography (TLC)**

TLC was performed on 10 cm × 20 cm dried aluminum-backed Silica Gel 60, F254 TLC plates (Merck, Darmstadt, Germany). In a fume hood, about 12.5 µg of each lipid sample and lipid standards in chloroform or chloroform - methanol (1:3, v/v) were deposited manually into 0.5 cm large bands and 0.8 cm apart from each other using a 25 µL solvent safe pipette tip. Development was carried out at room temperature in a sealable TLC glass chamber with chloroform – methanol – 30% ammoniac (65:35:5, v/v/v) used as the developing solvent.

The presence of different lipid classes was revealed either unspecifically with primulin reagent under 366 nm UV light (62.5 mg/L primulin in acetone- water, 8:2, v/v) or specifically with alpha-naphthol reagent for glycolipids (42) or with ninhydrin reagent for lipids containing free amino groups (43). In all cases, the separated bands of lipid samples were compared with the standard bands.

#### **High Performance Liquid Chromatography (HPLC)**

The HPLC analysis method was adapted from the work of Clavijo Rivera et al. (44).

Concretely, lipid fractions issued from SPE purification were analyzed by HPLC on a Uptisphere CS Evolution column (150 mm× 4.6 mm, 2.6 µm, 85 Å; Interchim, Montluçon, France). The system was composed of a modular UltiMate 3000 RS System (Dionex, Voisins Le Bretonneux, France) coupled with

an evaporative light scattering detector (ELSD) Sedex 85 (Sedere S.A., Alfortville, France). System control and data acquisition were handled using Chromeleon® Chromatography Management Software (Thermo Scientific).

About 5 – 10 µg of each lipid fraction in 10-20 µL of either chloroform or chloroform – methanol (1:3, v/v) were separately eluted using a solvent gradient from 100% A to 100% B where A was chloroform and B was a mixture of methanol – 30% ammonia solution – chloroform (92:7:1, v/v/v). The gradient started from 100% A to 80% A in 3 min, reduced in 9 min to 0% A and kept for 0.1 min. The column was finally equilibrated at 100% A for 2.9 min. The analysis was carried out at 30 °C with a flow rate of 1 mL/min. The ELSD temperature was set at 40 °C. The nebulizer gas pressure (dried and filtered air) was fixed at 3.2 bars and the photomultiplier sensitivity was set to a gain value of 6 (44).

The retention times of the separated peaks of the lipid classes were compared to those of the different lipid standards for the qualitative identification. Their estimated concentrations were obtained by using the calibration curves of the respective standards (44).

### **Gas Chromatography (GC)**

Fatty acid methyl esters (FAME) were prepared by direct esterification/transesterification of the fractions. In order to detect the eventual presence of the cyclopropane containing fatty acids, it was necessary to protect the cyclopropane cycle from the modifications caused by methylation reagents (45). Therefore, the methylation/transmethylation of our lipid extracts, classically performed with boron trifluoride (BF<sub>3</sub>, 14% in methanol) (45,46), has been performed simultaneously with trimethylsulfonium hydroxide (TMSH, ~ 0.25 M in methanol), which has been successfully used for this kind of compounds (12,13,47). The data obtained by the two approaches were similar.

*Methylation by TMSH:* For each sample, a suitable volume of lipid solution containing 200 µg of lipids in chloroform or chloroform – methanol (50:50, v/v) was collected in a 2 mL airtight glass vial. Methanol was then added to make 1 mg/mL solutions (*i.e.* to final volumes of 200 µL). 20 µL of TMSH was subsequently added. After 10 min of reaction, the samples were stored at -20°C until analysis by GC-FID (Flame Ionization Detector).

*Methylation by boron trifluoride-methanol:* the following analysis method was adapted from that proposed by Morrison et al. (46). For each sample, 15 µL of 1 mg/mL nonanoic acid (internal standard) in chloroform was added to 150 µg of lipids in a 15 mL airtight glass tube. The solvents were carefully evaporated under a nitrogen stream at RT. Then 1 mL of toluene and 1 mL of boron trifluoride-methanol solution were added to each tube. Tightly closed, the tubes were heated at 100 °C for 2, 10 and 30 min for fatty acid, phospholipid and glycolipid fractions respectively. The fractions were allowed to cool to RT. Then, after the addition of 1 mL of cyclohexane and 0.5 mL of water and a brief shaking of the solution, the fatty acid methyl ester

mixtures were extracted in the upper phase (46). The samples were stored at -20°C until analysis by GC-FID.

*GC-FID analysis:* Methylated samples were analyzed by GC using a Perkin Elmer Clarus 680 System equipped with a FID. The samples were injected in splitless mode and separated on a capillary column, coated with a polar stationary phase (DB-225, 30 m, 0.32 mm i.d., 0.25 µm). Hydrogen was used as carrier gas at a rate of 2 ml/min (hydrogen generator, F-DGSi, Evry, France). The temperature of the injector and the FID was set at 250°C. The program was as follows: the temperature was initially set at 50°C and kept constant for 1 minute. Then it increased linearly at a rate of 15°C/min to reach 180°C and was kept at this temperature for 1 minute. A second heating at a rate of 5°C/min brought the temperature to the final value of 220°, which was kept constant for 10 minutes.

Individual fatty acids were identified by comparison of their retention times with those of standards (FAME mix; Supelco, Sigma, France), while quantification was performed by determining the peak area ratio of the sample and the internal standard C9:0 fatty acid added during the methylation stage (48,49). The peak areas were corrected following the specific response factors of fatty acid methyl esters (48,49). Results were expressed as a percentage of each fatty acid (FA) to the total fatty acids (TFA) (g/100 g TFA).

#### **Supercritical-Fluid Chromatography – Electrospray Ionization – High Resolution Mass Spectrometry (SFC-ESI-HRMS)**

The samples were separated by supercritical-fluid chromatography using a 1260 Infinity Analytical SFC system (Agilent Technologies, Waldbronn, Germany). The system was composed of a controller module (G1170A), a SFC module (G4301A), a binary pump (G4302A), a degasser (G4225A), an auto sampler (G4303A) which was thermostated at 4°C and equipped with a 5 µL injection loop, a thermostatically controlled column compartment (G1316C), a UV-DAD detector (G1315C), a back pressure regulator BPR (G4301A), and a make-up isocratic pump (G1310B). T-union was placed in front of the BPR in order to split the mobile phase into two fractions, one fraction to BPR and the other one to MS. When coupling with a mass spectrometer, a caloritherm preheater (Sandra Selerity Technologies, Kortrijk, Belgium) set at 60°C was installed at the entrance of the ion source to avoid the freezing of the mobile phase. The SFC system was coupled with a 6540 Q-ToF mass spectrometer (Agilent Technologies, Waldbronn, Germany) fitted with electrospray (ESI dual JetStream).

Parameters were fixed for BPR at 130 bar and at 60°C. The mobile phase consisted of CO<sub>2</sub> (solvent A) and co-solvent (solvent B, 20 mM ammonium acetate in methanol - ethanol (1:1, v/v)). The program was as follows: 0 min, 1% B; 1.5 min, 4% B; 2.5 to 5.5 min, 15% B; 7.5 min, 30% B; 8.5 to 15 min, 45% B. A make-up solvent was added between the analytical column and the BPR. The make-up pump delivered a mixture of 20 mM ammonium acetate in methanol - ethanol (1:1, v/v) at 200 µL/min from 0 to 6 minutes,

then 100  $\mu\text{L}/\text{min}$  from 7 to 19 minutes. The samples were injected in full loop 5 $\mu\text{L}$  with overfill factor 3 and separated on diethanolamine packed column (Torus DEA, 2.1 mm x 100 mm x 1.7  $\mu\text{m}$ , Waters). Each lipid fractions were dissolved in chloroform - methanol (1:3, v/v) at a concentration of 0.1 mg/mL. The analysis was carried out at 60  $^{\circ}\text{C}$  with a flow rate of 0.9 mL/min.

Mass spectrometry (MS) parameters were set as follows: drying gas temperature 350 $^{\circ}\text{C}$ , Vcap 3500 V, fragmentor 160 V. Full-scan mode was employed in a range of  $m/z$  50-1700 at 2 GHz, giving a mass resolution higher than 25 000 at  $m/z$  922. Calibration solution containing two internal reference compounds, purine  $\text{C}_5\text{H}_4\text{N}_4$  at  $m/z$  121.0509 and HP-921 (hexakis (1H, 1H, 3H-tetrafluoropentoxy) phosphazene)  $\text{C}_{18}\text{H}_{18}\text{O}_6\text{N}_3\text{P}_3\text{F}_{24}$  at  $m/z$  922.0098, was continuously introduced resulting in mass accuracy below 5 ppm. Recorded data were analyzed with MassHunter Workstation B.08.00.

### **Nuclear Magnetic Resonance (NMR) spectroscopy**

Prior to the NMR analyses, samples were dissolved in 600 $\mu\text{L}$  of  $\text{CDCl}_3:\text{CD}_3\text{OD}$  (2:1) mixture (Euriso-TP, St Aubin F-91194, both chloroform and methanol purities were to 99.96% of deuterium atoms) and put in 5 mm tube matched for 9.4T spectrometer. NMR spectra were recorded on a Bruker 400 spectrometer drove with neo avance console, temperature was kept at 290K. Spectrometer was equipped with a 5 mm TXI ( $^1\text{H}, ^{13}\text{C}$ , X) probehead with proton and carbon frequencies of 400.33 and 100.66 MHz respectively. TMS was used as reference for proton and carbon ( $\delta\text{H}$ ,  $\delta\text{C}$  = 0). Both homo- and heteronuclear experiments were extracted from the Bruker library pulse sequences. Pulse, delay and power level were optimized for the two-dimensional homonuclear ( $^1\text{H}-^1\text{H}$ ) spectra (COSY90 and TOCSY) and the heteronuclear  $^1\text{H}-^{13}\text{C}$  (HSQC et HMBC) experiments. The data were exploited with the TopSpin software.

### **Monosaccharide analysis**

The sugar composition was determined by GC-FID following methanolysis and trimethylsilylation in comparison with authentic monosaccharide standards. Samples were methanolysed for 24h at 80 $^{\circ}\text{C}$  in 0.5M anhydrous MeOH-HCl prepared by adding acetyl chloride to anhydrous methanol (50). Solutions were neutralized by adding silver carbonate until pH 6-7. In order to eliminate fatty acid methyl esters, samples were washed twice with heptane ( $\rho$  = 0.684 g/mL) and the methanol ( $\rho$  = 0.791 g/mL) phases were dried under a stream of nitrogen. Methyl-glycosides were trimethylsilylated in 40  $\mu\text{L}$  bis-silyltrifluoroacetamide (BSTFA) in the presence of pyridine for 1 h at room temperature. Trimethyl-O-methylglycoside derivatives were injected in split mode in a gas chromatograph equipped with a capillary column (30 m X 0.25 mm) ID-SOLGEL-1MS 0.25  $\mu\text{m}$  (SGE GC-column); helium used as the carrier gas and the oven temperature program was 120 $^{\circ}\text{C}$  to 240 $^{\circ}\text{C}$  at 2 $^{\circ}\text{C}$  per min.

## **Matrix Assisted Laser Desorption/Ionization-Quadrupole Ion Trap (MALDI-QIT-TOF) analysis**

Native glycolipids and native standards (MGDG, DGDG) were resuspended in chloroform - methanol (1:2, v/v) to a final concentration of 1.6 mg/mL, then 1  $\mu$ L sample was mixed with 1  $\mu$ L of DHB matrix solution (10 mg/mL dissolved in chloroform/methanol 2:1, v/v) on MALDI plate.

MALDI-TOF mass spectra were acquired on MALDI-QIT-TOF Shimadzu AXIMA Resonance mass spectrometer (Shimadzu Europe, Manchester, UK) in positive mode. The mid mode (mass range  $m/z$  700-1100) was used with laser power set at 85 for 300 laser shots. For each spectrum MS and MS/MS recorded, 300 laser shots were performed and accumulated.

Structure assignment was made from calculated mass composition and fragmentation analysis on MS/MS spectrum.

### **Extraction of literature data and statistical analysis**

Our findings were compared with literature data selected according to the following procedure. In the search engine Web of Science™, the keywords bacteria, fatty acid, and composition were entered in the field “topic” and the search was extended over a large period (2022-1995). The articles have been sorted according to the following criteria:

- Bacteria (wild species, no mutants) produced with or without additives or peptides
- Lipid analysis on whole cells
- Right lipid attributions
- Complete data (articles giving the lipid composition with a sum less than 80% were discarded)
- In some cases, it is not clear whether cycC19:0 was detected or not or detected in a single band with another lipid (like C18:1). We took data as they were declared.

Older references found therein were added. In addition, we also considered the declarations provided in databanks like BacDive (<https://bacdiv.dsmz.de/>) to check or extend our search.

The data were curated as follows:

- Data below LOQ or LOD were put at 0
- The precision of data was harmonized with one digit
- As data are given with different levels of details (in particular due to the experimental conditions), we carried out groupings like, for example, C18:1 as a single entity for C18:1 cis 11, C18:1 cis 9...

Finally, a table was built with these data. It includes the original name of bacteria (as indicated in the article, underscore, a code related to the fermentation productions). In the next columns, the genus and species were checked and eventually modified according to the international Code of Nomenclature of Bacteria (51). Some reattributions were performed (for example *piscicola* to *maltaromaticum* and *Lactobacillus divergens*

into *Carnobacterium divergens*). As the amounts of unsaturated, saturated and cyclic fatty acids contents may be of importance for predicting or explaining the properties of bacteria (14), we have calculated these parameters as variables. In addition, we kept the most five representative fatty acids namely, C14:0, C16:0, C16:1, C18:0, C18:1 (Fig. S3). A Principal Component Analysis (PCA) was proceeded to these variables (5 fatty acids, unsaturated fatty acids (UFA), saturated fatty acids (SFA) and cyclic fatty acids (CFA)) using the statistical software R (52).

## Results

### Lipid classes of *C. maltaromaticum*

Lipids were extracted directly from the wet cells after freeze-thawing and washing. The total lipids which represented about 0.7% of the *C. maltaromaticum* CNCM I-3298 wet biomass corresponded to about 3.5% of the bacterial dry weight considering the ratio of dry weight to wet weight of bacterial cells (about 20%) (53). This amount was in the same order as the crude lipid extract reported for other lactic acid bacteria (1.8-7.5%) (20,54).

The crude lipid extract was fractionated on a SPE column in four fractions: 1 – chloroform fraction, 2 – chloroform-acetone fraction, 3 – acetone fraction, 4 – methanol fraction. These were examined by TLC (Fig. 1, A-B-C-D) and HPLC (Fig. 1E; SI, Fig. S1) in comparison with different lipid standards: oleic acid, monoolein, 1,2 and 1,3 dioleoyl-glycerol and trioleoyl glycerol (Sigma Aldrich mixture) for neutral lipids, MGDG and DGDG for glycolipids, DOPG/POPG, DOPS and lysoPE for phospholipids.

The chloroform fraction was shown to contain free fatty acids (FFA), and tri-glyceride (TG) (Fig. 1 A and B – lane 1, Fig. 1E – blue line, Fig. S1). The preponderance of FFA in this fraction was further confirmed by SFC-ESI-HRMS analysis (SI, Fig. S2).

The glycolipid nature of the chloroform – acetone and acetone fractions (Fig. 1A and B, lanes 2 and 3) were first suggested by comparison of their  $R_f$  values with ones of MGDG and DGDG then confirmed by the specific coloration by  $\alpha$ -naphthol stain of the eluted bands on the TLC plate. The HPLC chromatogram of the chloroform – acetone fraction showed two clearly distinguishable peaks (Fig.1E, green line). They were coherent with the two most visible bands of this fraction on TLC plates (Fig. 1A and B, lane 2). The minor peak at about 4.7 min, quite close to that of MGDG, might be attributed to a glycolipid with one hexose – the monohexaoyldiacylglycerols (MHDG). The major peak at 7.0 min was then tentatively identified as dihexaoyldiacylglycerols (DHDG) based on its retention time. In comparison to chloroform – acetone fraction, TLC and HPLC analyses showed that the acetone fraction was made of a single major compound

that co-eluted with DHDG (Fig. 1E, light-green line). Both fractions were further analyzed by mass spectrometry and NMR analyses (see section 3.3 Glycolipids of *C. maltaromaticum*).

For the methanol fraction, both TLC and HPLC analysis indicated that the most intense signal corresponded to phosphatidylglycerol phospholipids (PG) (Fig. 1A, B – line 4, 1E – red line). The other two HPLC peaks could presumably be phospholipids (55), here named phospholipid 1 (PL1) and phospholipid 2 (PL2) (Fig. 1E – red line). By comparing both the  $R_f$  values (Fig. 1C and D) and the characteristic violet color with the ninhydrin stain of these TLC bands (Fig. 1D), with those of LysoPE and DOPS standards (43), they were probably LysoPE and PS. In HPLC analysis, the retention times of these peaks were quite different from those of C18:1 LysoPE and DOPS standards suggesting that the nature of the fatty acid chains is different from C18:1. Using HPLC curve calibration, the phosphatidylphosphoglycerols (PG) were identified as the main constituents, about 93.7% (w/w).

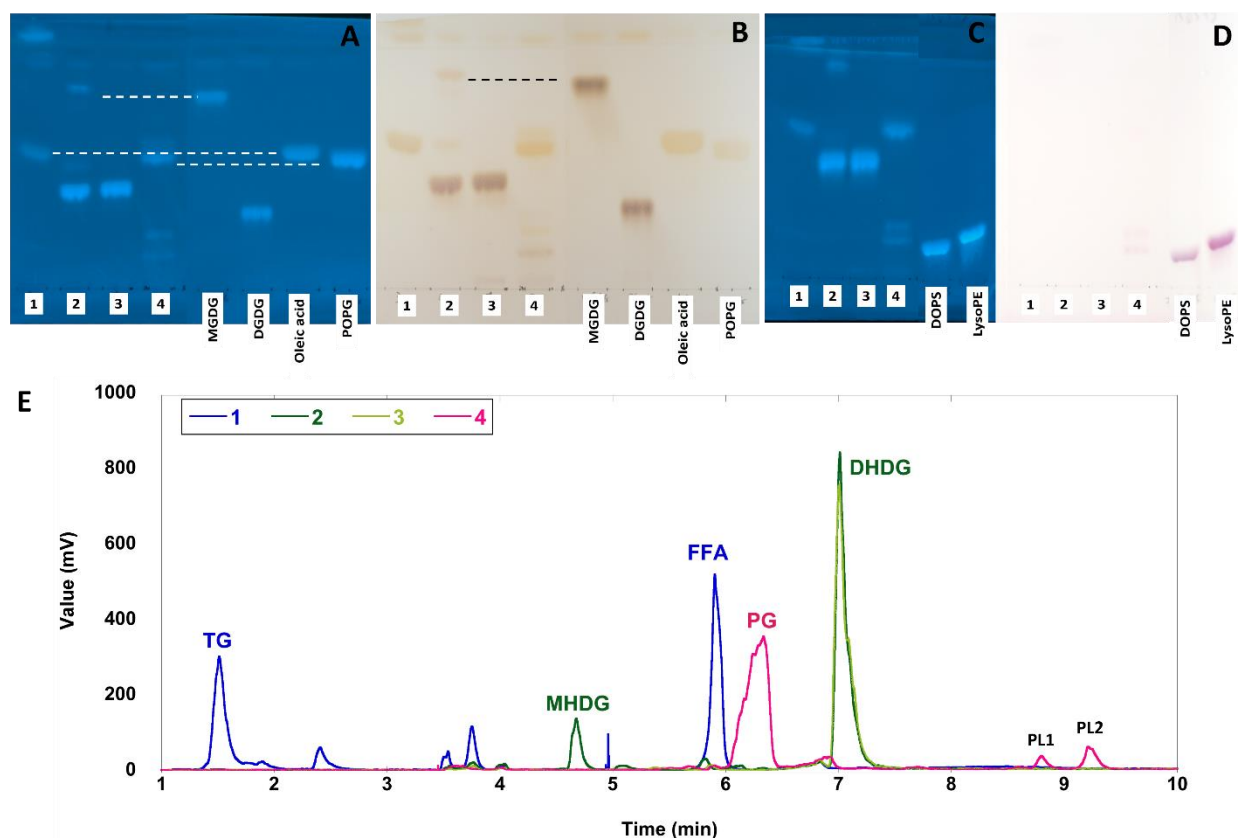


Figure 1: TLC (A-B-C-D) and HPLC (E) analysis of lipid fractions from *C. maltaromaticum* CNCM I-3298. The fractions are the following: 1= chloroform fraction, 2= chloroform-acetone fraction, 3= acetone fraction, 4= methanol fraction. (A-B-C-D) Silica gel aluminum coated TLC plates, developed with  $\text{CHCl}_3/\text{MeOH}/30\% \text{NH}_3$  (65/35/5, v/v/v) and revealed with (A, C) primulin stain and observed under 366 nm UV light; (B)  $\alpha$ -naphthol stain; (D) ninhydrin stain. Annotations above HPLC peaks indicate the nature of the respective bands: MHDG (Monohexaoyldiacylglycerol); DHDG (Dihexaoyldiacylglycerol); FFA (Free fatty acids); TG (Triglycerides); PL1 (Phospholipid 1, presumably LysoPE); PL2 (Phospholipid 2, presumably PS).

The composition of the membrane lipids of *C. maltaromaticum* CNCM I-3298 is shown in Table 1. The neutral lipids, phospholipids, and glycolipids represent 0.9, 3.9 and 2.2  $\mu\text{g}$  per mg of wet cells respectively.

Lipid fractions	$\mu\text{g}/\text{mg}$ wet weight	% (w/w)
Neutral lipids	$0.9 \pm 0.3$	$13.2 \pm 3.1$
Phospholipids	$3.9 \pm 0.1$	$54.8 \pm 0.4$
Glycolipids	$2.2 \pm 0.2$	$32.0 \pm 3.6$

Table 1: Amounts of lipids extracted from *C. maltaromaticum* CNCM I-3298 cultured in MN medium. (MN medium: medium composed of trehalose, proteose peptone, yeast extract, Tween 80,  $\text{MnSO}_4$ , and  $\text{MgSO}_4$  as detailed in (37))

Similarly to other LAB (19–21), glycolipids were present in a significant amount ( $32.0 \pm 3.6$  %, w/w) and constituted the second class of lipids present in *C. maltaromaticum* CNCM I-3298 after phospholipids ( $54.8 \pm 0.4$  %). Unexpectedly, the neutral lipid fraction (fraction 1) presented  $13.2 \pm 3.1$  % (w/w) of the total lipid extract. Its significant presence in the lipid extract of lactic acid bacteria was previously reported and even with a higher concentration, in the range of 40-60% for *L. plantarum* (56), and of 22.8-25.6% for *L. bulgaricus* NCS1 strain grown in different conditions with or without sodium oleate (9) (9,57). Until now, no explanation has been clearly stated by any authors. The presence of the fatty acid fraction may arise from the hydrolysis of phospholipids/glycolipids due to the inevitable release of lipases during the extraction.

#### **Phospholipids of *C. maltaromaticum***

The phospholipid fraction (methanol fraction) of *C. maltaromaticum* CNCM I-3298 was successfully identified by SFC-ESI-HRMS analysis (Fig. 2) (58). Annotation was performed according to the injection of standards determining the retention time range of each lipid subclass together with high mass precision measurements below 5 ppm. Finally, MS/MS experiments led to the identification of the fatty acid composition of the phospholipids. The methanol fraction containing phospholipid was first analyzed in positive and negative modes. In the positive ion mode, three signals related to phosphatidylglycerols (PG)  $[\text{M}+\text{NH}_4]^+$  ions were annotated at  $m/z$  792, 808 and 834 and four signals related to  $[\text{M}+\text{H}]^+$  ions were attributed at  $m/z$  749, 771, 775 and 797 (Fig. 2A). In the negative mode, PG predominantly formed  $[\text{M}+\text{H}]^-$  confirming data obtained in the positive ion mode (Fig. 2B).

The MS/MS spectrum of the precursor ion at  $m/z$  775 (Fig. 2C) confirms the glycerol head group according to the classical neutral loss of 172 amu leading to the fragment at  $m/z$  603. The fragment at  $m/z$  339 corresponds to the protonated C18:1 fatty acid plus 58 amu coming from a part of the glycerol according to the literature (59). In negative ion mode, the MS/MS spectrum of the precursor ion at  $m/z$  773 confirms the presence of a unique fatty acid according to the fragment at  $m/z$  281 (Fig. 2D). Thus, the signal of the ion at  $m/z$  775 can be attributed to the protonated phosphatidylglycerol PG (C18:1/C18:1) in the positive ion mode. Other signals were attributed according to mass difference with  $m/z$  775 and/or MS/MS data.

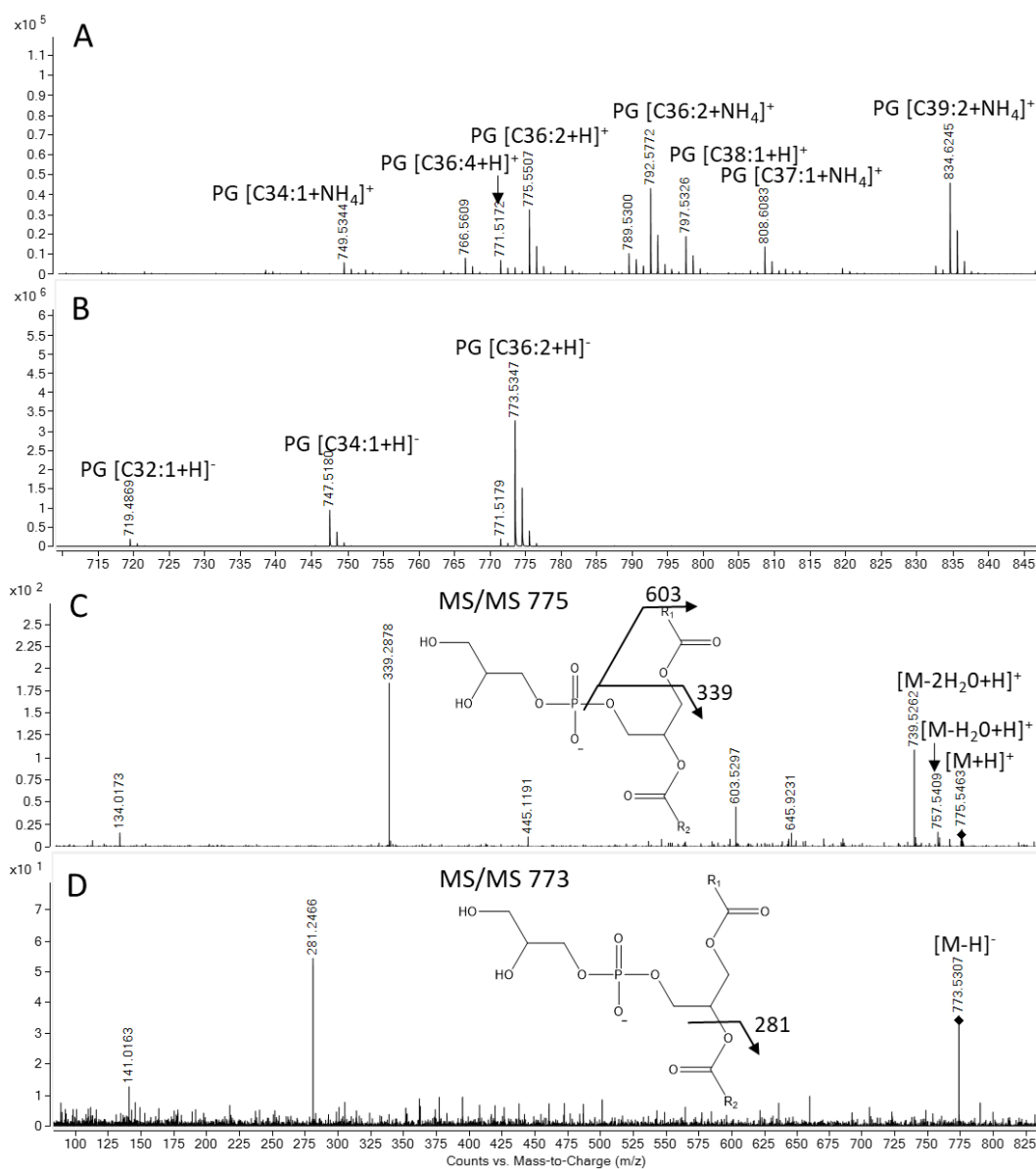


Figure 2: SFC-ESI-QTOF mass spectra of phospholipid fraction of *C. maltaromaticum* CNCM I-3298 in the positive (A) and negative (B) mode. (C) MS/MS spectrum of the precursor ions at  $m/z$  775 at 10eV collision energy in the positive ion mode. (D) MS/MS spectrum of the precursor ion at  $m/z$  773 at 30eV collision energy in the negative ion mode.

Although the presence of PS and LysoPE was suggested by TLC analysis, we could not detect their signal in MS analysis both in positive and negative modes. The explanation was that the quantities of both PL1 and PL2 were under the detection threshold.

Major fatty acids of phospholipids of *C. maltaromaticum* CNCM I-3298 were of the straight-chain monounsaturated and saturated types (C12 to C22) with mainly C18:1 (79%) and C16:0 (10%) fatty acid chains (Table 2). No cyclopropane fatty acids were detected. The UFA/SFA ratio was 5.0 which was

significantly higher than values available in the literature for phospholipids of other LAB, for example: 0.9-1.7 for *L. acidophilus*, 3.3 for *L. casei* (estimated from (60) and (61) respectively).

Fatty acid	Phospholipids (methanol fraction)	Glycolipids		Neutral lipids (chloroform fraction)
		Chloroform-acetone fraction	Acetone fraction	
C10:0	0.0	0.2	0.0	1.0
C12:0	0.4	0.3	0.2	1.2
C14:0	1.6	0.9	0.7	3.4
C14:1	0.1	0.1	0.0	0.3
C15:0	<b>0</b>	0.1	0.0	0.2
<b>C16:0</b>	<b>10.1</b>	<b>10.1</b>	<b>11.7</b>	<b>11.4</b>
C16:1	0.4	0.2	0.1	0.4
C17:0	0.1	0.1	0.0	0.0
C18:0	2.8	4.5	3.2	7.2
<b>C18:1</b>	<b>79.4</b>	<b>71.6</b>	<b>80.5</b>	<b>53.6</b>
C18:2n-6	0.3	1.0	0.1	0.5
C18:3n-3	0.6	0.5	0.1	0.3
C20:0	0.7	0.2	0.0	0.4
C20:1	0.2	0.2	0.0	0.3
C21:0	0.5	0.0	0.0	0.0
C22:0	0.4	0.5	0.1	1.1
C22:1	2.6	9.6	3.1	18.6
<b>UFA</b>	<b>83.4</b>	<b>83.2</b>	<b>84.1</b>	<b>74.0</b>
<b>SFA</b>	<b>16.6</b>	<b>16.8</b>	<b>15.9</b>	<b>26.0</b>
<b>UFA/SFA</b>	<b>5.0</b>	<b>4.9</b>	<b>5.3</b>	<b>2.8</b>

Table 2 : Fatty acid composition (% w/w) of phospholipids, glycolipids and neutral lipids extracted from *C. maltaromaticum* CNCM I-3298 cultured in MN medium. (MN medium: medium composed of trehalose, proteose peptone, yeast extract, Tween 80, MnSO<sub>4</sub>, and MgSO<sub>4</sub> as detailed in (37)). The individual lipid classes are methylated and analyzed by GC-FID. The separated peaks are attributed based on comparison of retention time with methylated fatty acid standards analyzed in the same conditions.

## Glycolipids of *C. maltaromaticum*

The glycolipid containing fractions (chloroform-acetone and acetone fractions) were analyzed by GC-FID, MS and MS/MS MALDI-QIT-TOF and NMR to determine the nature of sugars and fatty acid moieties associated to of each type of glycolipids.

The monosaccharide analysis by GC-FID (data not shown) showed that glycolipids contained both glucose (Glc) and galactose (Gal) with Gal:Glc ratios of 1.2-1.4 and 1.5-1.7 for the chloroform-acetone fraction and the acetone fraction respectively.

### 1.2.1. MALDI-QIT-TOF analysis

Subsequently, the molecular structure of these glycolipids was analyzed by MALDI-QIT-TOF in positive mode. In both cases, similar MS profiles were detected (Fig. 3A and 3B).

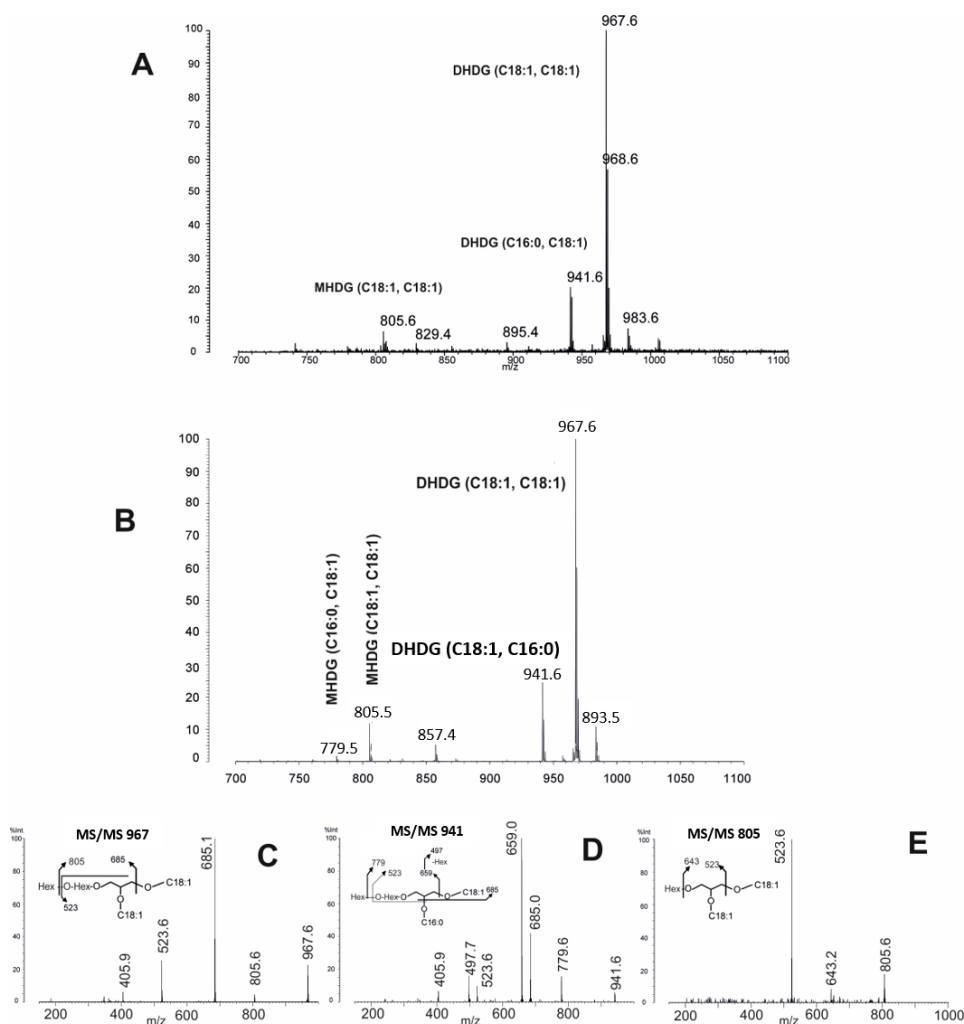


Figure 3: MALDI-QIT-TOF mass spectra in positive mode of (A) acetone and (B) chloroform-acetone fractions of *C. maltaromaticum* CNCM I-3298. (C, E) MS/MS analysis of signal at  $m/z$  967 and  $m/z$  805.6 from chloroform-acetone fraction. (D) MS/MS analysis of signals at  $m/z$  941.6 from acetone fraction. As inserts of pictures: (C-D) the molecular structure of DHDG: dihexaosyl (Glc/Gal) diacylglycerol, (E) the molecular structure of MHDG: monohexaosyl (Glc/Gal) diacylglycerol;  $m/z$  ions are identified with sodium adduct (i.e.  $[M+Na]^+$ ).

In chloroform-acetone and acetone fractions, three signals were observed at  $m/z$  967.6, 941.6 and 805.6 (Fig. 3A and 3B). They were identified by MS/MS analysis as dihexaoyldiacylglycerol [DHDG+Na]<sup>+</sup> with different fatty acid chains of C18:1-C18:1 and C18:1-C16:0 (Fig. 3C and 3D) and monohexaoyldiacylglycerol [MHDG+Na]<sup>+</sup> with C18:1-C18:1 fatty acid chains (Fig. 3E) as described below.

The MS/MS fragmentation of parent ions at  $m/z$  967.6, 941.6 and 805.6 generated [M-162+Na]<sup>+</sup> fragments at  $m/z$  805.6, 779.6 and  $m/z$  643.2, [M-282+Na]<sup>+</sup> fragments at  $m/z$  685.1, 659.0 and 523.6 as well as secondary fragments [M-282-162+Na]<sup>+</sup> fragments for two of them, which established the presence of at least one hexose in terminal non-reducing position and a C18:1 fatty acid in all three compounds. MS/MS fragmentation pattern of DHDG at  $m/z$  941.6 showed an additional [M-256+Na]<sup>+</sup> fragments ion at  $m/z$  685.0 (Fig. 3D), indicating the presence of a C16:0 fatty acid which confirmed that DHDG at  $m/z$  941.6 was substituted by a C18:1 and a C16:0 fatty acid chains, whereas DHDG at  $m/z$  967.6 was substituted by two C18:1. The predominance of the fragment at  $m/z$  659.0 compared to 685.0 indicated the positional distribution of the acyl groups: C18:1 at *sn*-1 and the C16:0 at *sn*-2 of the glycerol backbone (62). Finally, the signal at  $m/z$  805 was attributed to [MHDG+Na]<sup>+</sup> with the C18:1-C18:1 fatty acid chains (Fig. 3E). Its MS/MS profile showed fragments of  $m/z$  643.2 and 523.6 which corresponded respectively to the loss of one hexose ([M-162+Na]<sup>+</sup>) or a loss of a C18:1 chain ([M-282+Na]<sup>+</sup>). The minor signal at  $m/z$  983 was attributed to [DHDG+K]<sup>+</sup> C18:1-C18:1 adduct. The minor signal at  $m/z$  779.5 (Fig. 3B) was attributed to [MHDG+Na]<sup>+</sup> adduct with two fatty acyl chains of C16:0 and C18:1. Other minor signals at  $m/z$  829.4 and 895.4 (Fig. 3A) and 857.4 (Fig. 3B) were not successfully attributed to glycolipid related adducts and though be assigned as contaminants.

The relative intensities of different signals observed in MALDI-MS spectra suggested that DHDG was more abundant than MHDG (Fig. 2 A and B). The quantities of MHDG and DHDG were then estimated by HPLC analysis using standard curves of glycolipid standards (MGDG, DGDG). The results showed that MHDG represented approximately 5% compared to 95% (w/w) for DHDG in the total glycolipids. NMR analysis also confirmed these values with at least 93.5 % of DHDG (w/w) and less than 6.5% (w/w) of MHDG. Furthermore, the DHDG with two fatty acid chains of C18:1 seemed to be predominant compared to DHDG with C18:1-C16:0 fatty acid chains (Fig. 3A and 3B).

To clarify the structure of the glycolipids and identify the exact nature of their glycan moieties, compounds were analyzed by NMR.

### **NMR analysis**

In order to determine the sequence, including linkage and configuration of the monosaccharides of the glycolipids, a series of NMR experiments was recorded (Fig. 4, 5 and Table S1, S2).

As shown in Fig. 4, the chloroform-acetone and acetone fractions exhibited similar  $^1\text{H-NMR}$  spectra indicating very close compositions, which were confirmed by heteronuclear  $^1\text{H-}^{13}\text{C}$  HSQC analysis (not shown). The two fractions only differed by the presence of two minor anomeric signals at  $\delta^1\text{H} = 4.83$  (acetone fraction, Fig. 4, top) and 5.13 (chloroform-acetone fraction, Fig. 4, bottom) and of an additional  $-\text{CH}_2\text{OH}$  signal at  $\delta^1\text{H} = 3.64$  ( $\delta^{13}\text{C} = 70.2$  on HSQC spectrum) in the chloroform-acetone fraction that was identified as a polyethylene glycol contamination (Fig. 4, arrow).

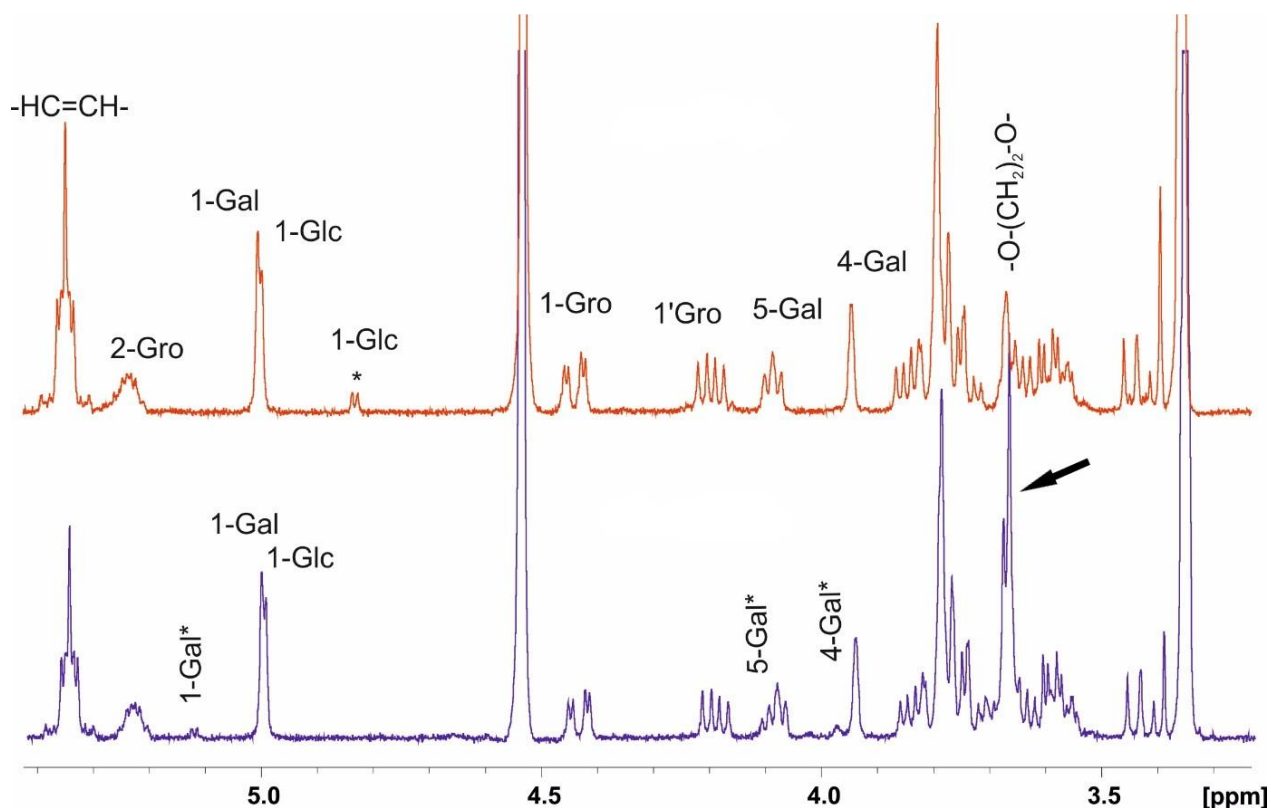


Figure 4: Parts of  $^1\text{H-NMR}$  spectra of glycolipids from acetone fraction (top) and glycolipids from chloroform-acetone fraction (bottom) of *C. maltaromaticum* CNCM I-3298. Gro: Glycerol. \* related monosaccharide from minor glycolipids. The black arrow refers to a signal of  $-\text{O}-(\underline{\text{CH}_2})_2\text{-O}-$ .

In chloroform-acetone and acetone fractions, we identified two superimposable anomeric  $^1\text{H-}^{13}\text{C}$  signals at 5.00-96.70 ppm corresponding to two different spin systems (Fig. 5, Table S1). NMR parameters of glycolipids in the acetone fraction were fully established by  $^1\text{H-}^{13}\text{C}$  HSQC (Fig. 5),  $^1\text{H-}^1\text{H}$  COSY, TOCSY and ROESY NMR analyses (not shown). Two different spin systems attributed to  $\alpha\text{Glc}$  and  $\alpha\text{Gal}$  residues were identified from the single anomeric signal at  $\delta$  5.00/96.70 (Fig. 5) in accordance with monosaccharide analysis by GC-FID and literature (20). The  $\alpha$ -configuration of both Glc and Gal residues was confirmed by the value of the direct heteronuclear coupling constant  $^1J_{\text{C,H}}$  of anomeric signal at 169 Hz, as observed on the undecoupled  $^1\text{H-}^{13}\text{C}$  HSQC (not shown).

The spin system of the  $\alpha$ -Glc established by the combination of  $^1\text{H}$ - $^1\text{H}$  TOCSY and  $^1\text{H}$ - $^{13}\text{C}$  HSQC analyses showed that the chemical shift of its C2 was significantly downfielded at 76.6 ppm compared to an unsubstituted, indicating that  $\alpha$ -Glc residue was substituted in C2 position (Fig. 5, Table S1). In contrast, C3, C4 and C6 carbons observed at 72.0, 69.9 and 61.40 ppm respectively, which were identified as unsubstituted carbons (Fig.5, Table S1), unambiguously identified this residue as a C2-substituted  $\alpha$ -Glc residue, in agreement with literature (20,63).

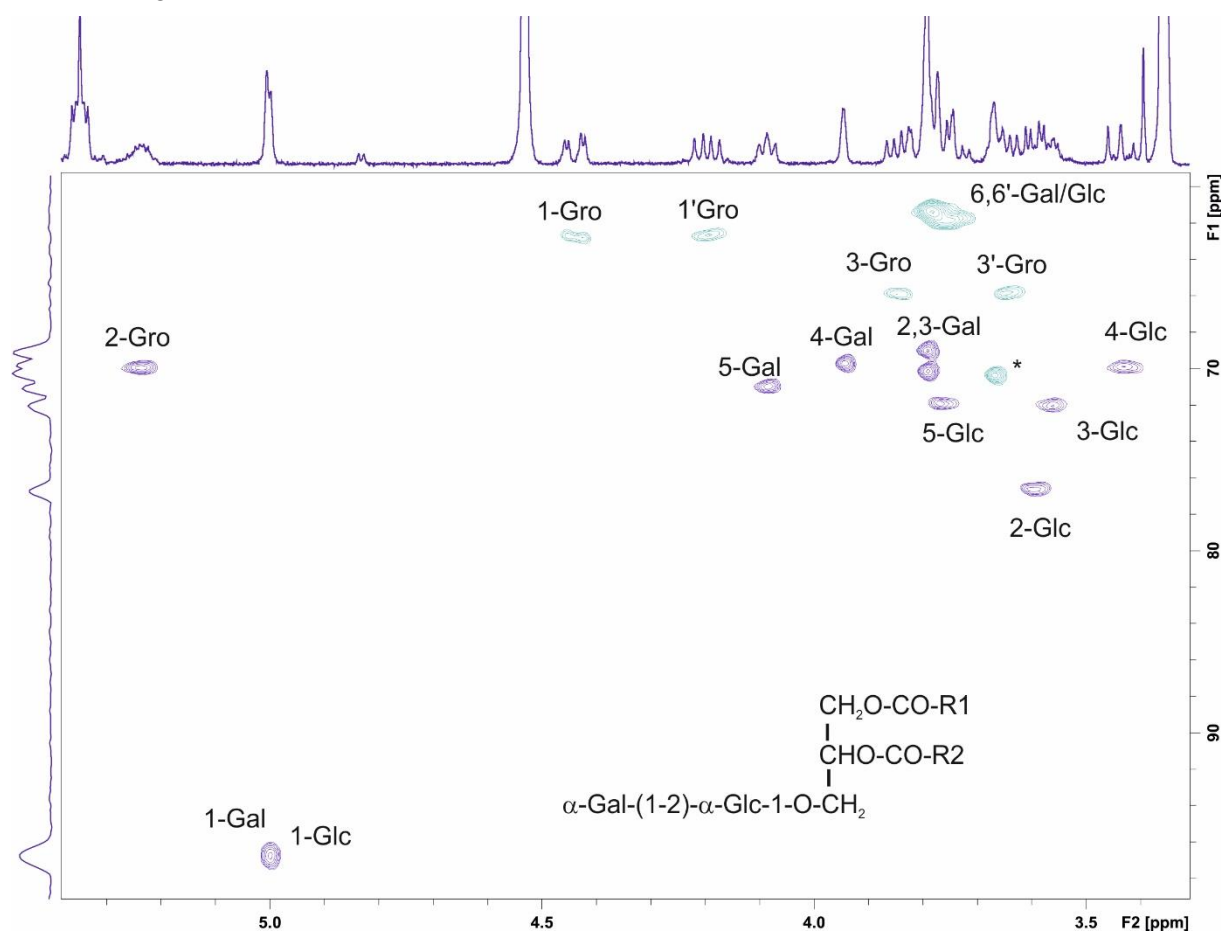


Figure 5: Part of  $^1\text{H}$ - $^{13}\text{C}$  HSQC experiment of glycolipids from acetone fraction of *C. maltaromaticum* CNCM I-3298. \* signal from  $-\text{O}-(\text{CH}_2)_2-\text{O}-$

The second spin-system originating from the  $^1\text{H}$ - $^{13}\text{C}$  anomeric signal at 5.00/96.7 ppm was unambiguously identified as an  $\alpha$ -Gal residue based on the set of  $^3J_{\text{H1,H2}}$ ,  $^3J_{\text{H2,H3}}$ ,  $^3J_{\text{H3,H4}}$  and  $^3J_{\text{H4,H5}}$  correlation values (S/L/S/S). Moreover, the H5 that was identified as a deshielded multiplet at 4.08/71.0 ppm (Fig.5, Table S1) confirmed this identification (20,63,64). In contrast to the C2-substituted  $\alpha$ -Glc residue, none of its constituted carbons showed deshielded NMR chemical shifts, which established that this residue was an  $\alpha$ -Gal residue at the unreducing end position of the molecule. In addition to the two monosaccharide residues, HSQC spectrum showed another spin system attributed to a fully substituted glycerol (Fig. 5, Table S2).

Indeed, the split H1,H1'-C1 signal at 4.44/4.19-62.70 ppm, as well as the H2-C2 signal at 5.23/69.95 ppm, clearly indicated that both C1 and C2 positions of glycerol (Gro) were esterified by fatty acid groups, as typically observed in such glycolipids. In contrast, the H3,H3'-C3 signals at 3.84/3.65-65.9 ppm indicated that the C3 position was O-substituted by a sugar residue. This observation was confirmed by nuclear Overhauser effect (NOE) effect between H1 of Glc residue with both H3, H3' of Gro on the ROESY spectrum (Fig. not shown). Altogether, multidimension NMR analyses demonstrated that the major component of both chloroform-acetone and acetone fractions was a glycolipid with the following structure  $\alpha$ -Gal(1,2)- $\alpha$ -Glc-O-Gro in which Gro is esterified at both C1 and C2 positions.

Finally, both additional minor signals observed at 5.13 and 4.83 ppm in chloroform-acetone and acetone fractions respectively were identified thanks to homonuclear  $^1\text{H}$ - $^1\text{H}$  COSY and TOCSY experiments (data not shown).

In chloroform-acetone fraction, the anomeric signal at 5.13 ppm (Fig. 4, bottom) that resonated as a doublet with homonuclear vicinal coupling constant ( $^3J_{\text{H1,H2}}$ ) of 3.6 Hz was identified as having  $\alpha$ -Galacto configuration (65). TOCSY spectrum (not shown) indicated that H1 was coupled with H2 signal which resonated as a quadruplet at 3.53 ppm ( $^3J_{\text{H2,H1}} = 3.6$  Hz and  $^3J_{\text{H2,H3}} = 9.4$  Hz). The H2 itself coupled with a quadruplet H3 signal resonating at 3.79 ppm and exhibiting one large and one small coupling constants. Moreover, this H3 was itself correlated with H4 resonating as a pseudo singlet at 3.95 ppm with two very small coupling constants (i.e.  $^3J_{\text{H4,H3}}$  and  $^3J_{\text{H4,H5}} \ll 5$ Hz). Finally, the slightly downfield shift of H5 confirming the attribution as an  $\alpha$ -galactosyl residue completed this information. So, the  $^1\text{H}$  spin system typified the minor glycolipid in this fraction as mono-galactosyl-diacylglycerol. Similarly, the anomeric signal at 4.83 ppm (Fig. 4, top) in the acetone fraction which resonated with a small homonuclear vicinal coupling constant ( $^3J_{\text{H1,H2}} = 3.9$ Hz) was identified as an unsubstituted  $\alpha$ -Glc which strongly suggested that this fraction contained a mono-glucosyl-diacylglycerol.

Thus, the combination of mass spectrometry, NMR and GC-FID analyses showed clearly that the glycolipids of *C. maltaromaticum* CNCM I-3298 were essentially  $\alpha$ -Gal-(1-2)- $\alpha$ -Glc-diglycerides along with the minor ones,  $\alpha$ -Gal-diglycerides and  $\alpha$ -Glc-diglycerides.

#### **GC-FID analysis**

Finally, the fatty acid composition of all the glycolipid fractions was analyzed by GC-FID. The results obtained by the two methods of methylation were consistent and shown in Table 2.

Glycolipids of *C. maltaromaticum* CNCM I-3298 contained essentially fatty acids of the straight-chain monounsaturated and saturated types (C10 to C22) with predominant C18:1 (71-80%) and C16:0 (10-12%) fatty acid chains. These results confirmed the dominance of C18:1 chain vs C16:0 and their preponderance in the glycolipid samples as observed in the MS spectra (Fig. 2A and B). No cyclopropane fatty acids were

observed. The UFA/SFA ratio of these glycolipids was 4.9-5.3, significantly higher than reported values for glycolipids of other LAB (*L. plantarum*, *L. casei* and *L. acidophilus*: 1.2-2.8) (19,20,66).

### Neutral lipids of *C. maltaromaticum*

As observed for the polar lipids, the fatty acids were essentially straight-chain monounsaturated and saturated types (C10 to C20) with mainly C18:1 (53%) and C16:0 (11%) fatty acid chains (Table 2). No cyclopropane fatty acids were detected.

The neutral lipid fraction of *C. maltaromaticum* CNCM I-3298 was rich in free fatty acids and triglycerides (Fig. 1 A, B, E, Fig. S1). Other components of this fraction were mainly diglycerides (DG) as demonstrated by SFC-ESI-HRMS in negative and positive modes (Fig. S2). The fatty acid composition of these DG was also revealed by SFC-ESI-HRMS analysis (Fig. 6). The most intense signals at  $m/z$  638 (Fig. 6A) can be attributed to the ammonium adduct of DG 36:2, which is consistent with the fatty acid composition of the neutral lipids. The annotation was confirmed by MS/MS experiments. The precursor ion at  $m/z$  638 led to the unique fragment in the low mass range at  $m/z$  339 which is characteristic of the loss of the fatty acid C18:1 from the protonated fragment at  $m/z$  621 (Fig. 6). Thus, the molecular structure of DG is mainly C18:1-C18:1.

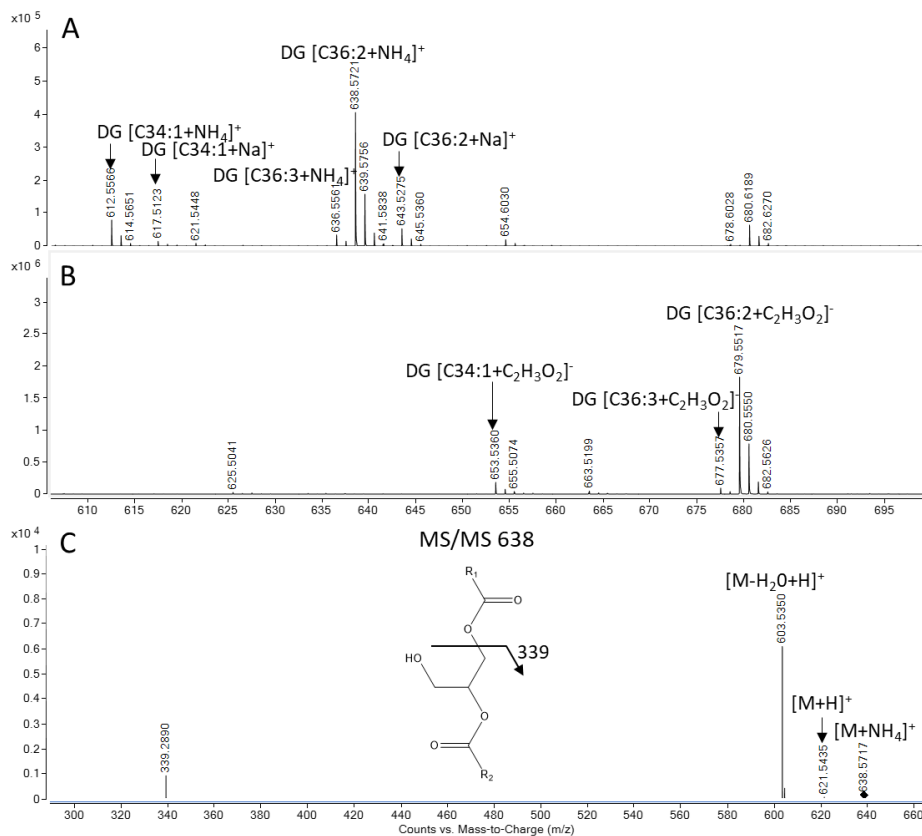


Figure 6: SFC-ESI-QTOF mass spectra of diglycerides (DG) of *C. maltaromaticum* CNCM I-3298 in the positive (A) and negative (B) mode. (C) MS/MS spectrum of the precursor ion at  $m/z$  638 at 10eV collision energy in the positive ion mode.

## Discussion

Our study shows that the cytoplasmic membrane of *C. maltaromaticum* CNCM I-3298 was mainly composed of glycerophospholipids (54.8%) and glyceroglycolipids (32.0%) (Fig. 7A). Within glycolipids, the quantity of DHDG was about 95% (w/w) compared to about 5% (w/w) for MHDG (Fig. 7C). This predominance of glycerophospholipids and glyceroglycolipids and especially the feature rich in DHDG over MHDG have been encountered on many gram-positive bacteria (19,21,67). We did not observe the presence of tri- and tetra-hexaacyldiacylglycerol in *C. maltaromaticum* CNCM I-3298. In the literature, for LAB, their presence was only observed in *Lactobacillus* species (19–21,60). The nature of sugars found in *C. maltaromaticum* CNCM I-3298 is simple: galactose and glucose. MHDG was found with either galactose or glucose while DHDG has the same structure as DHDG found in *Lactobacillus* species, *i.e.*  $\alpha$ -Gal-(1-2)- $\alpha$ -Glc-diglycerides (19,20,68). This is, however, the first time that this sugar structure is found in *Carnobacterium* genus. According to MALDI-MS analysis, the most abundant molecular species were C18:1-C18:1 followed by C18:1-C16:0 fatty acid containing DHDG and C18:1-C18:1 containing fatty acid for MHDG. In some other LAB, the major molecular species of MHDG and DHDG contained C18:1 (n-9 or n-11) -C19:0 cyclopropane fatty acids (19,20).

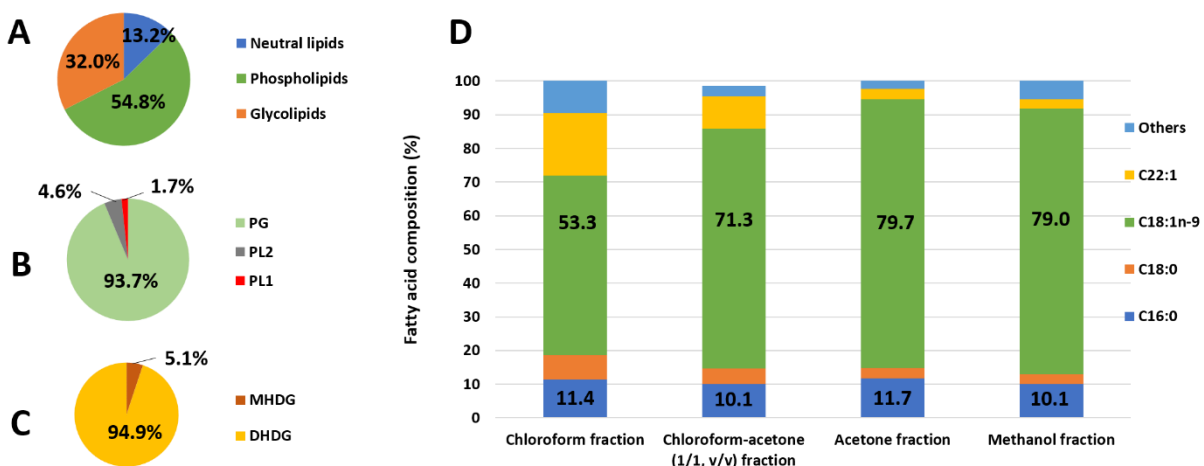


Figure 7: Lipids of *C. maltaromaticum* I-3298 cultured in MN medium: A) Different lipid classes (Neutral lipids, Phospholipids and Glycolipids), B) Phospholipids (PG, PL1 (presumably LysoPE) and PL2 (presumably PS)), C) Glycolipids (MHDG and DHDG) and D) Fatty acid composition. 1= chloroform fraction, 2= chloroform-acetone fraction, 3= acetone fraction, 4= methanol fraction.

Despite some similarities with other LAB, *C. maltaromaticum* CNCM I-3298 also has several specificities. First, phosphatidylphosphoglycerol (PG) is nearly the sole constituent among the phospholipid class, with about 93.7% (w/w) (Fig. 7B). This property is remarkable as compared to other LAB (55-68% in *Lactobacillus* spp.) (67,69) or other gram-positive bacteria such as *Staphylococcus aureus* (57%), *Bacillus subtilis* (70%) (70). Second, we found much higher oleic acid contents in *C. maltaromaticum* than those found in many LAB (9,11–13,71–74) and these results are significantly higher than those reported for *C.*

*maltaromaticum* (23,74): about 75% (w/w) for whole cellular fatty acids compared to about 49-54% previously reported (71,73,74). Conversely, we found slightly lower C16:0 amounts in *C. maltaromaticum* CNCM I-3298 (about 10% vs 14-18%) and only minor quantities of C14:0 and C16:1 acids (less than 4% in our cases compared to 10-18% previously reported) (23,73,74). As a consequence, the UFA/SFA ratios of polar lipids of *C. maltaromaticum* CNCM I-3298 for each lipid class were between 4.9 to 5.3. Third, no cyclopropane containing fatty acids were found in *C. maltaromaticum* CNCM I-3298, in accordance with other studies about *Carnobacterium* (23,26,73,74). The particular high content of oleic acid of *C. maltaromaticum* CNCM I-3298 found in this study and in the study of Girardeau et al. 2021 (82.6%) (26) can be explained by two factors: inherent properties of the bacterium and external conditions. On the one hand, psychrophilic bacteria such as *Carnobacterium*, generally have a higher content of unsaturated fatty acids in comparison with thermophilic bacteria (75,76). Among them, even in non-oleate culture medium, *C. maltaromaticum* naturally have higher oleic acid content compared to other strains (23,74). This point will be further demonstrated by our PCA analysis. On the other hand, bacterial fatty acid composition is strongly affected by the fermentation conditions, such as pH (9,77–79), temperature (78,80,81), harvest time (81) and especially fermentation composition (5,9,78,82,83). In particular, the oleic acid content could arise drastically with the presence of oleic acid supplement (Tween 80 or sodium oleate for example) in the culture medium (5,9,83,84) as in this study.

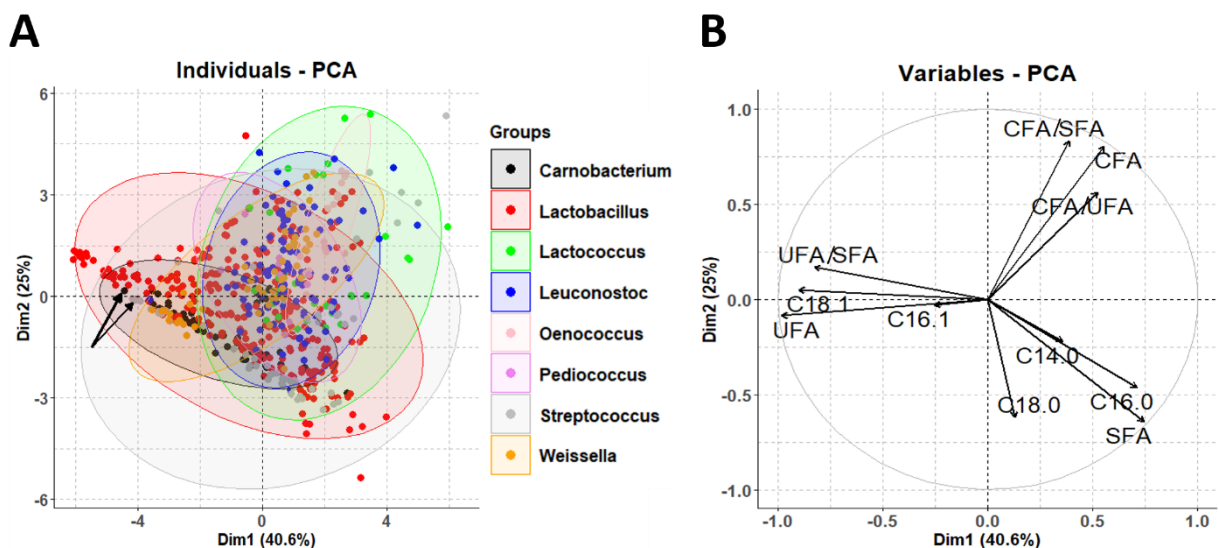


Figure 8: Principal component analysis of the main fatty acid compositions of the lipid membranes of bacteria. (A) Graph of individuals with each point representing a bacterial composition, coloured according to the genus. The arrows refer to *C. maltaromaticum* CNCM I-3298 from our study (in bold) and from Girardeau et al (26) (in thin). Ellipses group 95% of points in a genus. (B) Graph of variables.

To confirm the specificities of *C. maltaromaticum* CNCM I-3298 within the lactic acid bacteria family, fatty acid compositions of lactic acid bacteria have been compiled from a systemic bibliographic search (see section 2.11: Extraction of literature data and statistical analysis and reference (87) for the dataset including our findings). Because cyclic fatty acids have been reported to be a key element in the cryoresistance of lactic acid bacteria (5,9,12), we integrated them as a single component in the analysis, in addition to the four common major fatty acids C14:0, C16:0, C16:1 and C18:1. The five selected fatty acids usually account for more than 70% of total fatty acids. We compiled the proportions of these fatty acids for many lactic acid bacteria (627 compositions), whatever the strains and their culture conditions (medium, pH, temperature, agitation, harvesting time). We calculated the UFA, SFA and CFA contents as well as ratios UFA/SFA, CFA/UFA and CFA/SFA. A principal component analysis was performed with the whole dataset (Fig. 8) and for the sole *Carnobacterium* genus (Fig. 9).

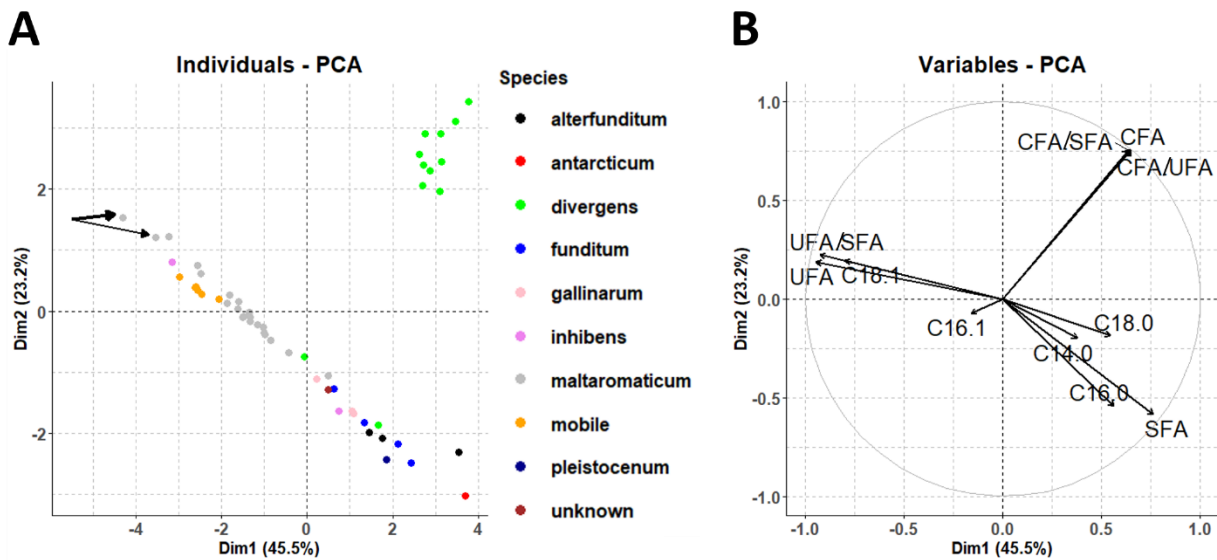


Figure 9: Principal component analysis of the main fatty acid compositions of lipid membranes of *Carnobacterium* genus. (A) Graph of individuals with each point representing a bacterial composition, coloured according to the species. (B) The graph of variables. The arrows refer to *C. maltaromaticum* CNCM I-3298 from our study (in bold) and from Girardeau et al (26) (in thin).

The two first components explain about 65% of the variance and thus, are good representatives of the system (Fig. 8). The graph of variables indicates a direction for UFA, another one for CFA and a third direction for SFA (Fig. 8B). Fig. 8A confirms that *C. maltaromaticum* CNCM I-3298 is one of the richest bacteria in terms of UFA among the *Carnobacterium* genus (placed along the axis for UFA) and the *Carnobacterium* genus is poor in cyclic fatty acid. A closer look at the *Carnobacterium* family (Fig. 9A and B), highlights that the strain *divergens* is the only specie among *Carnobacterium* that is able to produce cyclic fatty acids. Fig. 8 also highlights that some bacteria are very rich in cyclic fatty acids (like *Lactococcus*, *Leuconostoc* and *Oenococcus*) and the variation in their lipid composition is essentially related to the modulation of cyclic fatty acid production. The strains of *Streopococcus* and *Lactobacillus* do not give any clear trend so all types

from highly saturated, to unsaturated and cyclic are found. The variation within the *Weissella* genus essentially relates to the unsaturated and cyclic fatty acids. Overall, this PCA shows that *C. maltaromaticum* CNCM I-3298 has a peculiar fatty acid composition in comparison to other strains. As this bacterium shows exceptional cryoresistance and the fatty acid composition was one of the key elements in this property, the cryoresistance of bacteria in the vicinity of *C. maltaromaticum* CNCM I-3298 could be interesting to go deeper in the understanding of structure-cryoresistance relationships in bacteria. Such study should wisely include the analysis of glycolipids. Literature is rich in bacterial fatty acid composition and its relationship to cryoresistance, attributing a positive role to the unsaturated fatty acid content and also for some of them, to the cyclic fatty acids. However, a thorough characterization of bacteria lipids membranes, such as this work, is lacking in literature and seems worth studying for better understanding the role of lipid membranes in bacteria freeze-thawing resistance. We speculated based on literature (17,86) that the glycolipids could give some kind of order and robust structure to the membrane, thus contributing to the cryoresistance. Deep characterization of strains presenting different cryoresistance is needed to conclude on what makes *C. maltaromaticum* so cryoresistant (or on markers of cryoresistance).

In conclusion, the lipid membrane of *C. maltaromaticum* CNCM I-3298 is rich in UFA (C18:1, 70-80% in polar lipids), phosphatidylglycerol (55% whose 94% is phosphatidylglycerol) and glycolipids dihexaoyldiglyceride (32% with 95% of dihexaoyldiglyceride) with mainly  $\alpha$ -Gal(1-2)- $\alpha$ -Glc as sugar. Neither cardiolipin, nor cyclic fatty acid were identified. This work gives light on the detailed composition of a highly freeze-resistant micro-organisms and proposes that together with the higher content of UFA, which provides a high degree of fluidity to the membrane (85), phosphatidylglycerol as main phospholipids and the presence of significant content of glycolipids could also be markers of cryo-resistance.

### **Data availability statement**

Most of the data presented in this manuscript except for the SFC-ESI-HRMS data was deposited on the repository Recherche.Data.Gouv. in appropriate formats which respect the FAIR principles. They can be found with this provisional private link: <https://entrepot.recherche.data.gouv.fr/privateurl.xhtml?token=969d079f-b5e1-4709-98ee-4e6fb5357c79>.

The authors engage to complete the dataset as soon as possible before the final publication of the accepted version.

### **Supporting information**

This article contains supporting information.

### **Acknowledgements**

We thank Dr D. Ropartz (INRAE, BIA, BIBS, F-44316, Nantes, France) for the useful suggestions. We thank the PAGés platform (US 41 - UAR 2014 - PLBS, France) for the analysis of glycolipids (GC-FID, MALDI-QIT-TOF-MS, and acquisition/interpretation of NMR analyses) and the NMR platform from Institut Chevreul (Université de Lille) for the NMR spectrometer. We thank Stéphanie Cenard (Université Paris-Saclay, INRAE, AgroParisTech, UMR SayFood, F-91120 Palaiseau, France) for the preparation of *C. maltaromaticum* CNCM I-3298 concentrates.

### **Author's contributions**

HPT, AR and MHR conceived and designed the analysis. MHR supervised the project, performed the fatty acid composition review and the statistical analysis. HPT, MHR, EM, WZ and DT wrote the manuscript. HPT carried out the lipid extraction/isolation and analysis by TLC. CC, EM, YG, FK, NY performed the MS, NMR and constituent analysis of glycolipids. WZ, DT performed the MS analysis of phospholipid and neutral lipids. AK and MV performed the HPLC and GC analysis of all the lipid fractions. AG and FF identified the *C. maltaromaticum* CNCM I-3298 production conditions for this study. AG performed the production of one batch of *C. maltaromaticum* CNCM I-3298. All authors reviewed the final manuscript.

### **Funding**

This project has received funding from the European Union's Horizon 2020 research and innovation program under grant agreement N° 777657. This project was also supported by grants from Région Ile-de-France (DIM Analytics) and by the Agence Nationale de la Recherche (Grant ANR-16-CE29-0002-01 CAP-SFC-MS). The authors would also like to thank BPI France and Région Ile-de-France for their financial support to the LIPOCOSM2 project through the French FUI grant.

### **Conflicts of interest**

The authors declare that they have no conflicts of interest with the contents of this article.

## References

1. Florou-Paneri P, Christaki E, Bonos E. Lactic Acid Bacteria as Source of Functional Ingredients. In: Christaki E, editor. Rijeka: IntechOpen; 2013. p. Ch. 25. Available from: <https://doi.org/10.5772/47766>
2. Marco ML, Heeney D, Binda S, Cifelli CJ, Cotter PD, Foligné B, et al. Health benefits of fermented foods: microbiota and beyond. *Curr Opin Biotechnol*. 2017;44:94–102.
3. Fonseca F, Béal C, Corrieu G. Operating conditions that affect the resistance of lactic acid bacteria to freezing and frozen storage. *Cryobiology*. 2001;43(3):189–98.
4. Carvalho AS, Silva J, Ho P, Teixeira P, Malcata FX, Gibbs P. Relevant factors for the preparation of freeze-dried lactic acid bacteria. *Int Dairy J*. 2004;14(10):835–47.
5. Goldberg I, Eschar L. Stability of lactic acid bacteria to freezing as related to their fatty acid composition. *Appl Environ Microbiol*. 1977;33(3):489–96.
6. Elliott GD, Wang S, Fuller BJ. Cryoprotectants: A review of the actions and applications of cryoprotective solutes that modulate cell recovery from ultra-low temperatures. *Cryobiology* [Internet]. 2017;76:74–91. Available from: <http://dx.doi.org/10.1016/j.cryobiol.2017.04.004>
7. Wang G, Yu X, Lu Z, Yang Y, Xia Y, Lai PFH, et al. Optimal combination of multiple cryoprotectants and freezing-thawing conditions for high lactobacilli survival rate during freezing and frozen storage. *Lwt* [Internet]. 2019;99(September 2018):217–23. Available from: <https://doi.org/10.1016/j.lwt.2018.09.065>
8. Vecchio C. Freeze-Drying Process: Principle and Practice. *Pharm Technol Dev* [Internet]. 2010;1–120. Available from: <http://users.unimi.it/gazzalab/wordpress/wp-content/uploads/2011/12/54-Liofilizzazione.pdf>
9. Smittle RB, Gilliland SE, Speck ML, Walter WM. Relationship of Cellular Fatty Acid Composition to Survival of *Lactobacillus bulgaricus* in Liquid Nitrogen I. *Appl Microbiol*. 1974;27(4):738–43.
10. Peter M. Cryobiology: The freezing of biological systems. *Science* (80- ). 1970;138(3934):939–949.
11. Zavaglia AG, Disalvo EA, De Antoni GL. Fatty acid composition and freeze-thaw resistance in lactobacilli. *J Dairy Res*. 2000;67(2):241–7.
12. Gautier J, Passot S, Pénicaud C, Guillemin H, Cenard S, Lieben P, et al. A low membrane lipid phase transition temperature is associated with a high cryotolerance of *Lactobacillus delbrueckii* subspecies *bulgaricus* CFL1. *J Dairy Sci* [Internet]. 2013;96(9):5591–602. Available from: <http://linkinghub.elsevier.com/retrieve/pii/S0022030213004682>
13. Meneghel J, Passot S, Dupont S, Fonseca F. Biophysical characterization of the *Lactobacillus delbrueckii* subsp. *bulgaricus* membrane during cold and osmotic stress and its relevance for cryopreservation. *Appl Microbiol Biotechnol* [Internet]. 2017;101(4):1427–41. Available from: <http://dx.doi.org/10.1007/s00253-016-7935-4>
14. Fonseca F, Pénicaud C, Tymczynszyn EE, Gómez-Zavaglia A, Passot S. Factors influencing the membrane fluidity and the impact on production of lactic acid bacteria starters. *Appl Microbiol Biotechnol*. 2019;103(17):6867–83.
15. Kociurzynski R, Pannuzzo M, Böckmann RA. Phase Transition of Glycolipid Membranes Studied by Coarse-Grained Simulations. *Langmuir*. 2015;31(34):9379–87.
16. Shipley GG, Green JP, Nichols BW. (Received February 23rd, 1973). 1973;311:531–44.

17. Yamakawa T, Nagai Y. Glycolipids at the cell surface and their biological functions. *Trends Biochem Sci.* 1978;3(2):128–31.
18. Hölzl G, Dörmann P. Structure and function of glycoglycerolipids in plants and bacteria. *Prog Lipid Res.* 2007;46(5):225–43.
19. Iwamori M, Sakai A, Minamimoto N, Iwamori Y, Tanaka K, Aoki D, et al. Characterization of novel glycolipid antigens with an  $\alpha$ -galactose epitope in lactobacilli detected with rabbit anti-Lactobacillus antisera and occurrence of antibodies against them in human sera. *J Biochem.* 2011;150(5):515–23.
20. Sauvageau J, Ryan J, Lagutin K, Sims IM, Stocker BL, Timmer MSM. Isolation and structural characterisation of the major glycolipids from *Lactobacillus plantarum*. *Carbohydr Res [Internet].* 2012;357:151–6. Available from: <http://dx.doi.org/10.1016/j.carres.2012.05.011>
21. Shaw N. Bacterial glycolipids. *Bacteriol Rev.* 1970;34(4):365–77.
22. Mora D, Scarpellini M, Franzetti L, Colombo S, Galli A. Reclassification of *Lactobacillus maltaromicus* (Miller et al. 1974) DSM 20342T and DSM 20344 and *Carnobacterium piscicola* (Collins et al. 1987) DSM 20730T and DSM 20722 as *Carnobacterium maltaromaticum* comb. nov. *Int J Syst Evol Microbiol.* 2003;53(3):675–8.
23. Collins M, Farrow J, Phillips B, Ferusu S, Jones D. Classification of *Lactobacillus divergens*, *Lactobacillus piscicola*, and Some Catalase-Negative, Asporogenous, Rod-Shaped Bacteria from Poultry in a New Genus *Carnobacterium*. *Int J Syst Bacteriol.* 1987;37(4):310–6.
24. Leisner JJ, Laursen BG, Prévost H, Drider D, Dalgaard P. *Carnobacterium*: Positive and negative effects in the environment and in foods. *FEMS Microbiol Rev.* 2007;31(5):592–613.
25. Walker VK, Palmer GR, Voordouw G. Freeze-thaw tolerance and clues to the winter survival of a soil community. *Appl Environ Microbiol.* 2006;72(3):1784–92.
26. Girardeau A, Passot S, Meneghel J, Cenard S, Lieben P, Trelea I-C, et al. Insights into lactic acid bacteria cryoresistance using FTIR microspectroscopy. *Anal Bioanal Chem.* 2022;414:1425–43.
27. Laursen BG, Bay L, Cleenwerck I, Vancanneyt M, Swings J, Dalgaard P, et al. *Carnobacterium divergens* and *Carnobacterium maltaromaticum* as spoilers or protective cultures in meat and seafood: Phenotypic and genotypic characterization. *Syst Appl Microbiol.* 2005;28(2):151–64.
28. Afzal MI, Jacquet T, Delaunay S, Borges F, Millière JB, Revol-Junelles AM, et al. *Carnobacterium maltaromaticum*: Identification, isolation tools, ecology and technological aspects in dairy products. *Food Microbiol [Internet].* 2010;27(5):573–9. Available from: <http://dx.doi.org/10.1016/j.fm.2010.03.019>
29. Larrouture-Thiveyrat C, Pepin M, Leroy-Sétrin S, Montel MC. Effect of *Carnobacterium piscicola* on aroma formation in sausage mince. *Meat Sci.* 2003;
30. Zhang P, Badoni M, Gänzle M, Yang X. Growth of *Carnobacterium* spp. isolated from chilled vacuum-packaged meat under relevant acidic conditions. *Int J Food Microbiol [Internet].* 2018;286(May):120–7. Available from: <https://doi.org/10.1016/j.ijfoodmicro.2018.07.032>
31. Spanu C, Piras F, Mocci AM, Nieddu G, De Santis EPL, Scarano C. Use of *Carnobacterium* spp protective culture in MAP packed Ricotta fresca cheese to control *Pseudomonas* spp. *Food Microbiol.* 2018;74:50–6.
32. Koné AP, Zea JMV, Gagné D, Cinq-Mars D, Guay F, Saucier L. Application of *Carnobacterium maltaromaticum* as a feed additive for weaned rabbits to improve meat microbial quality and safety. *Meat Sci [Internet].* 2018;135(January 2017):174–88. Available from: <https://doi.org/10.1016/j.meatsci.2017.09.017>

33. Stiles ME, Carlson D, Smith DC. Enhanced preservation of processed food [Internet]. US 9066521 B2, 2015. Available from: <https://patents.google.com/patent/US9066521B2/en>
34. EFSA CEF Panel (EFSA Panel on Food Contact Materials, Enzymes F and PA. Scientific Opinion on the safety evaluation of a time-temperature indicator system, based on *Carnobacterium maltaromaticum* and acid fuchsin for use in food contact materials. EFSA J [Internet]. 2013;11(7). Available from: <http://doi.wiley.com/10.2903/j.efsa.2010.1928>
35. Ellouze M, Pichaud M, Bonaiti C, Coroller L, Couvert O, Thuault D, et al. Modelling pH evolution and lactic acid production in the growth medium of a lactic acid bacterium: Application to set a biological TTI. *Int J Food Microbiol* [Internet]. 2008;128(1):101–7. Available from: <http://dx.doi.org/10.1016/j.ijfoodmicro.2008.06.035>
36. Girardeau A, Biscola V, Keravec S, Corrieu G, Fonseca F. Application of Lactic Acid Bacteria in Time-Temperature Integrators : A Tool to Monitor Quality and Safety of Perishable Foods. In: *Lactic Acid Bacteria* [Internet]. 1st Editio. CRC Press; 2020. Available from: <https://www.taylorfrancis.com/chapters/edit/10.1201/9780429422591-14/application-lactic-acid-bacteria-time-temperature-integrators-amélie-girardeau-vanessa-biscola-sophie-keravec-georges-corrieu-fernanda-fonseca>
37. Girardeau A, Puentes C, Keravec S, Peteuil P, Trelea IC, Fonseca F. Influence of culture conditions on the technological properties of *Carnobacterium maltaromaticum* CNCM I-3298 starters. *J Appl Microbiol*. 2019;126(5):1468–79.
38. Kates M. Bacterial Lipids. In: Paoletti R, Kritchevsky DBT-A in LR, editors. Elsevier; 1964. p. 17–90. Available from: <http://www.sciencedirect.com/science/article/pii/B978148319938250008X>
39. Salton M. Structure and function of bacterial cell membranes. *Annu Rev Microbiol*. 1967;21(February):417–22.
40. Bligh E., Dyer W. A rapid method of total lipid extraction and purification. *Can J Biochem Physiol*. 1959;37(8):911–7.
41. Kates M. Lipid extraction procedures. In: *Techniques of Lipidology*. Elsevier Science & Technology Books; 1982. p. 347–53.
42. Wang Z, Benning C. *Arabidopsis thaliana* polar glycerolipid profiling by thin layer chromatography (TLC) coupled with gas-liquid chromatography (GLC). *J Vis Exp*. 2011;(49):2–7.
43. Christie WW, Han X. *Lipid analysis*. THE OILY PRESS; 2010. 101 p.
44. Clavijo Rivera EP. Etude physicochimique du comportement d'une solution synthétique d'un broyat de microalgues et de la séparation par procédés membranaires des lipides qu'il contient [Internet]. Université de Nantes; 2017. Available from: <http://www.theses.fr/2017NANT4099/document>
45. Christie WW. Preparation of Lipid Extracts From Tissues. In: *Advances in Lipid Methodology*. Oily Press. 1993. p. 195–213.
46. Morrison WR, Smith LM. Preparation of Fatty Acid Methyl Esters and Dimethylacetals From Lipids. *J Lipid Res*. 1964;5(1 3):600–8.
47. Müller K-D, Husmann H, Nalik HP, Schomburg G. Trans-esterification of fatty acids from microorganisms and human blood serum by trimethylsulfonium hydroxide (TMSH) for GC analysis. *Chromatographia*. 1990;30(5–6):245–8.
48. Ulberth F, Gabernig RG, Schrammel F. Flame-Ionization Detector Response to Methyl, Ethyl, Propyl, and Butyl Esters of Fatty Acids. *JAOCS, J Am Oil Chem Soc*. 1999;76(2):263–6.
49. Ackman RG, Sipos JC. Application of specific response factors in the gas chromatographic analysis

- of methyl esters of fatty acids with flame ionization detectors. *J Am Oil Chem Soc.* 1964;41(5):377–8.
50. Liu KS. Preparation of fatty acid methyl esters for gas-chromatographic analysis of lipids in biological materials. *J Am Oil Chem Soc.* 1994;71(11):1179–87.
  51. Parte AC, Carbasse JS, Meier-Kolthoff JP, Reimer LC, Göker M. List of prokaryotic names with standing in nomenclature (LPSN) moves to the DSMZ. *Int J Syst Evol Microbiol.* 2020;70(11):5607–12.
  52. R Core Team. R: A language and environment for statistical computing. R Foundation for Statistical Computing, Vienna, Austria [Internet]. 2022. p. URL <https://www.r-project.org/>. Available from: <https://www.r-project.org/>
  53. Bratbak G, Dundas I. Bacterial dry matter content and biomass estimations. *Appl Environ Microbiol.* 1984;48(4):755–7.
  54. Ikawa M. Nature of the lipids of some lactic acid bacteria. *J Bacteriol.* 1963;85:772-781.
  55. Kates M. Separation of lipid mixtures. In: *Techniques of lipidology.* Elsevier Science & Technology Books; 1982. p. 393–469.
  56. Desens C, Lonvaud-Funel A. Etude de la constitution lipidique des membranes de bactéries lactiques utilisées en vinification. *Connaiss Vigne Vin.* 1988;22(1):25–32.
  57. Desens C, Lonvaud-Funel A. Etude de la constitution lipidique des membranes de bactéries lactiques utilisées en vinification. *Connaiss Vigne Vin.* 1988;22(1):25–32.
  58. Chollet C, Boutet-Mercey S, Laboureur L, Rincon C, Méjean M, Jouhet J, et al. Supercritical fluid chromatography coupled to mass spectrometry for lipidomics. *J Mass Spectrom.* 2019;54(10):791–801.
  59. Hsu FF, Turk J. Studies on glycerophospholipids with triple quadrupole tandem mass spectrometry with electrospray ionization: Structural characterization and fragmentation processes. *Am Soc Mass Spectrom* [Internet]. 2001;12(9):1036–43. Available from: <https://www.sciencedirect.com/science/article/pii/S1044030501002859>
  60. Fernández Murga ML, Cabrera G, Martos G, Font De Valdez G, Seldes AM. Analysis by mass spectrometry of the polar lipids from the cellular membrane of thermophilic lactic acid bacteria. *Molecules.* 2000;5(3):518–9.
  61. Thorne KJI. The phospholipids of *Lactobacillus casei*. *BBA - Spec Sect Lipids Relat Subj.* 1964;84(3):350–3.
  62. Fuchs B, Süß R, Schiller J. An update of MALDI-TOF mass spectrometry in lipid research. *Prog Lipid Res* [Internet]. 2010;49(4):450–75. Available from: <http://dx.doi.org/10.1016/j.plipres.2010.07.001>
  63. Toukach P V., Egorova KS. Carbohydrate structure database merged from bacterial, archaeal, plant and fungal parts. *Nucleic Acids Res.* 2016;44(D1):D1229–36.
  64. Egorova KS, Toukach PV. Carbohydrate Structure Database (CSDB): Examples of Usage. In: Aoki-Kinoshita K (eds), editor. *A Practical Guide to Using Glycomics Databases* [Internet]. Springer, Tokyo; 2017. p. 75–113. Available from: [https://link.springer.com/chapter/10.1007/978-4-431-56454-6\\_5#citeas](https://link.springer.com/chapter/10.1007/978-4-431-56454-6_5#citeas)
  65. Koerner TAW, Prestegard JH, Yu RK. Oligosaccharide Structure by Two-Dimensional Proton Nuclear Magnetic Resonance Spectroscopy. *Methods Enzymol* [Internet]. 1987;138(18):38–59. Available from: <https://pubmed.ncbi.nlm.nih.gov/3600333/>

66. Fernández Murga M, Cabrera G, Font De Valdez G, Disalvo A, Seldes A. Influence of growth temperature on cryotolerance and lipid composition of *Lactobacillus acidophilus*. *J Appl Microbiol*. 2000;88(2):342–8.
67. Kato S, Tobe H, Matsubara H, Sawada M, Sasaki Y, Fukiya S, et al. The membrane phospholipid cardiolipin plays a pivotal role in bile acid adaptation by *Lactobacillus gasseri* JCM1131 T. *Biochim Biophys Acta - Mol Cell Biol Lipids* [Internet]. 2019;1864(3):403–12. Available from: <https://doi.org/10.1016/j.bbalip.2018.06.004>
68. Paściak M, Górska S, Jawiarczyk N, Gamian A. *Lactobacillus johnsonii* glycolipids, their structure and immunoreactivity with sera from inflammatory bowel disease patients. *Microb Biotechnol*. 2017;10(2):456–68.
69. Drucker DBB, Megson G, Harty DWSWS, Riba I, Gaskell SJJ. Phospholipids of *Lactobacillus* spp. *J Bacteriol*. 1995;177(21):6304–8.
70. Malanovic N, Lohner K. Antimicrobial peptides targeting Gram-positive bacteria. Vol. 9, Pharmaceuticals. 2016.
71. Collins M, Farrow J, Phillips B, Ferusu S, Jones D. Classification of *Lactobacillus divergens*, *Lactobacillus piscicola*, and Some Catalase-Negative, Asporogenous, Rod-Shaped Bacteria from Poultry in a New Genus, *Carnobacterium*. *Int J Syst Bacteriol*. 1987;37(4):310–6.
72. Streit F, Delettre J, Corrieu G, Béal C. Acid adaptation of *Lactobacillus delbrueckii* subsp. *bulgaricus* induces physiological responses at membrane and cytosolic levels that improves cryotolerance. *J Appl Microbiol*. 2008;105(4):1071–80.
73. Ringø E, Seppola M, Berg A, Olsen RE, Schillinger U, Holzapfel W. Characterization of *Carnobacterium divergens* strain 6251 isolated from intestine of Arctic charr (*Salvelinus alpinus* L.). *Syst Appl Microbiol*. 2002;25(1):120–9.
74. Kim DH, Austin B. Characterization of probiotic carnobacteria isolated from rainbow trout (*Oncorhynchus mykiss*) intestine. *Lett Appl Microbiol*. 2008;47(3):141–7.
75. Chan M, Himes RH, Akagi JM. Fatty acid composition of thermophilic, mesophilic, and psychrophilic clostridia. *J Bacteriol*. 1971;106(3):876–81.
76. Russell NJ, Fukunaga N. A comparison of thermal adaptation of membrane lipids in psychrophilic and thermophilic bacteria. *FEMS Microbiol Lett*. 1990;75(2–3):171–82.
77. Gilliland SE, Speck ML. Relationship of cellular components to the stability of concentrated lactic *Streptococcus* cultures at -17°C. *Appl Microbiol*. 1974;27(4):793–6.
78. Guerzoni ME, Lanciotti R, Cocconcelli PS. Alteration in cellular fatty acid composition as a response to salt, acid, oxidative and thermal stresses in *Lactobacillus helveticus*. *Microbiology*. 2001;147(8):2255–64.
79. Broadbent JR, Larsen RL, Deibel V, Steele JL. Physiological and transcriptional response of *Lactobacillus casei* ATCC 334 to acid stress. *J Bacteriol*. 2010;192(9):2445–58.
80. Murga MLF, Cabrera GM, Font De Valdez G, Disalvo A, Seldes AM, Fernández Murga ML, et al. Influence of growth temperature on cryotolerance and lipid composition of *Lactobacillus acidophilus*. *J Appl Microbiol*. 2000;88(2):342–8.
81. Velly H, Bouix M, Passot S, Penicaud C, Beinstener H, Ghorbal S, et al. Cyclopropanation of unsaturated fatty acids and membrane rigidification improve the freeze-drying resistance of *Lactococcus lactis* subsp. *lactis* TOMSC161. *Appl Microbiol Biotechnol*. 2015;99(2):907–18.
82. To TMH, Grandvalet C, Tourdot-Maréchal R. Cyclopropanation of membrane unsaturated fatty

- acids is not essential to the acid stress response of *Lactococcus lactis* subsp. *cremoris*. *Appl Environ Microbiol.* 2011;77(10):3327–34.
83. Johnsson T, Nikkila P, Toivonen L, Rosenqvist H, Laakso S. Cellular fatty acid profiles of *Lactobacillus* and *Lactococcus* strains in relation to the oleic acid content of the cultivation medium. *Appl Environ Microbiol.* 1995;61(12):4497–9.
  84. Nikkilä P, Johnsson T, Toivonen L, Rosenqvist H. The effect of Tween 80 on the fatty acid composition of *Lactobacillusbuchneri* and *Lactobacillus brevis*. *J Gen Appl Microbiol.* 1995;41(4):327–32.
  85. Girardeau A, Passot S, Meneghel J, Cenard S, Lieben P, Trelea IC, et al. Insights into lactic acid bacteria cryoresistance using FTIR microspectroscopy. *Anal Bioanal Chem.* 2022;414(3):1425–43.
  86. Curatolo W. Glycolipid function William. *Biochim Biophys Acta* [Internet]. 1987;906:137–60. Available from: papers2://publication/uuid/A114E9A4-E3E9-4E2C-BD74-2BAC4A4422B8
  87. [dataset] HP. Ta, C. Clarisse, E. Maes, N. Yamakawa, Y. Guérardel, F. Krzewinski, W. Zarzycka, D. Touboul, A. Girardeau, F. Fonseca, A. Kermarrec, M. Viau, A. Riaublanc, MH. Ropers. (2023) Membrane lipid composition of *Carnobacterium maltaromaticum* CNCM I-3298, a highly cryoresistant lactic bacterium. *Recherche.Data.Gouv. Provisional Version*, <https://doi.org/10.57745/ZEXQUI>

## Supporting information

### Membrane lipid composition of *Carnobacterium maltaromaticum* CNCM I-3298, a highly cryoresistant lactic bacterium

HP. Ta<sup>1,\*</sup>, C. Clarisse<sup>2</sup>, E. Maes<sup>2</sup>, N. Yamakawa<sup>2</sup>, Y. Guérardel<sup>3,4</sup>, F. Krzewinski<sup>3</sup>, W. Zarzycka<sup>5</sup>, D. Touboul<sup>5</sup>, A. Girardeau<sup>6</sup>, F. Fonsec<sup>6</sup>, A. Kermarrec<sup>1</sup>, M. Viau<sup>1</sup>, A. Riaublanc<sup>1</sup>, MH. Ropers<sup>1</sup>

<sup>1</sup> : INRAE, BIA, F-44316, Nantes, France

<sup>2</sup> : Univ. Lille, CNRS, INSERM, CHU Lille, Institut Pasteur de Lille, US 41-UAR 2014-PLBS, F-59000 Lille, France

<sup>3</sup> : Univ. Lille, CNRS, UMR 8576 - UGSF - Unité de Glycobiologie Structurale et Fonctionnelle, F-59000 Lille, France

<sup>4</sup> : Institute for Glyco-core Research (iGCORE), Gifu University, Gifu, Japan

<sup>5</sup> : Université Paris-Saclay, CNRS, Institut de Chimie des Substances Naturelles, UPR 2301, 91198, Gif-sur-Yvette, France.

<sup>6</sup> : Université Paris-Saclay, INRAE, AgroParisTech, UMR SayFood, AgroParisTech, INRAE, Université Paris-Saclay, Thiverval-Grignon, France

\*: corresponding author, [haphuong.ta@inrae.fr](mailto:haphuong.ta@inrae.fr)

### List of Supporting Information

*Figure S1: HPLC analysis of lipid fractions from C. maltaromaticum CNCM I-3298. The fractions are the following: 1= chloroform fraction, 2= chloroform-acetone fraction, 3= acetone fraction, 4= methanol fraction. (A) 4 fractions compared to standards of oleic acid, MGDG (Monogalactosyldiacylglycerol), DGDG (Digalactosyldiacylglycerol), DOPG (1,2-Dioleoyl-sn-glycero-3-phospho-(1'-rac-glycerol)) and TG (triglycerides); (B) chloroform fraction compared to neutral lipid standards: MG, DG and TG (Mono-, Di- and Tri- glycerides) and FFA (free fatty acid).*

*Figure S2: LC-MS analysis of the chloroform fraction of lipids of C. maltaromaticum CNCM I-3298 showing the presence of free fatty acids (FFA), triglycerides (TG) and diglycerides (DG). ESI total ion chromatogram in the positive (A) and in the negative (B) ion mode. (C) Zoom on the FFA peak. (D) MS signal of principal FFA in the negative ion mode. PEG (Polyethyleneglycol signal was attributed to contaminants).*

*Figure S3: Number of studies corresponding to the sum of the proportion of the five fatty acids (C14:0, C16:0, C16:1, C18:1 and cycC19:0) ranged in class.*

*Table S1: Chemical shifts (ppm) observed in HSQC experiments of acetone fraction*

*Table S2: Chemical shifts (ppm) observed in HSQC experiments for glycerol signals from acetone fraction*

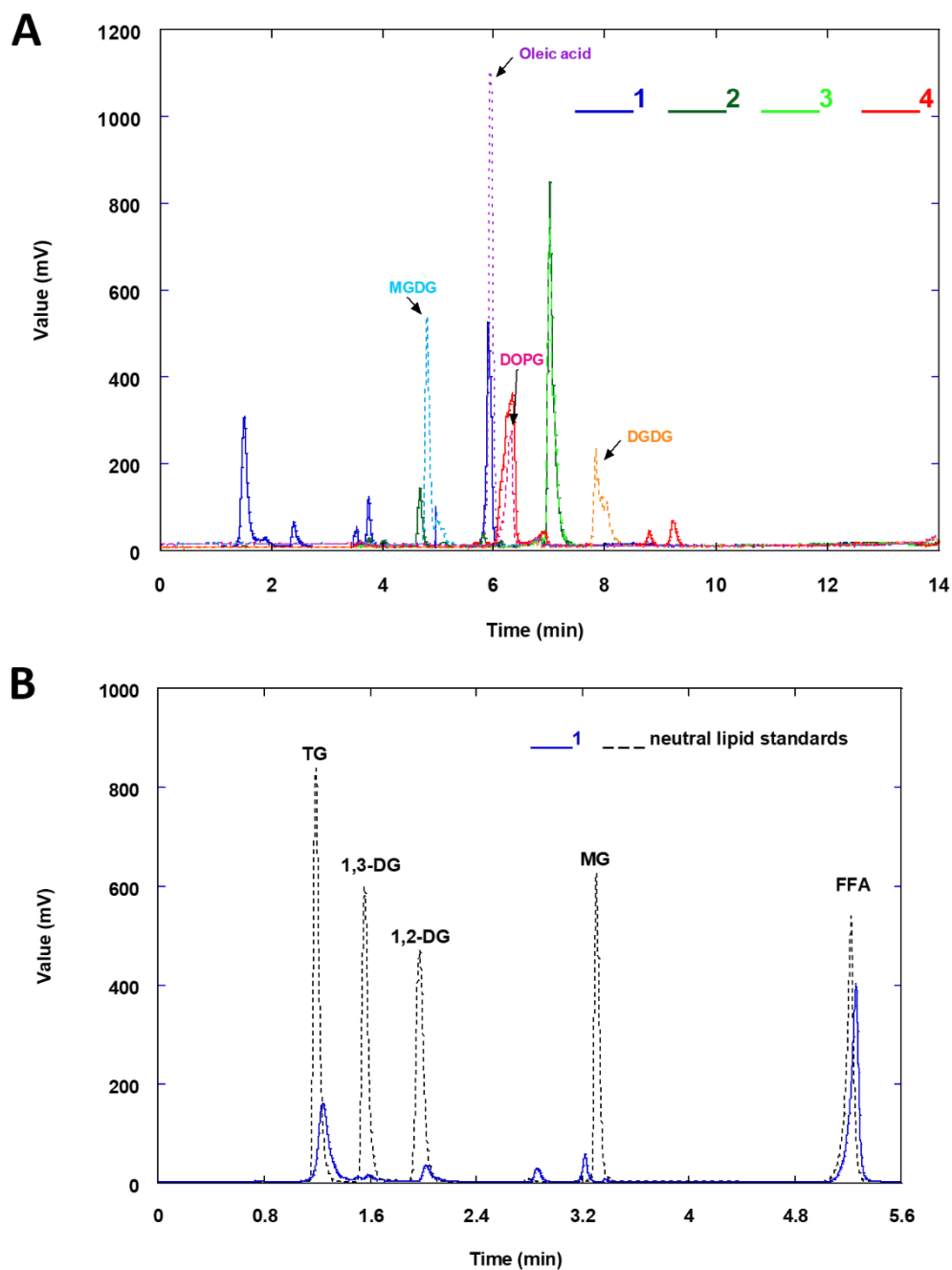


Figure S1: HPLC analysis of lipid fractions from *C. maltaromaticum* CNCM I-3298. The fractions are the following: 1= chloroform fraction, 2= chloroform-acetone fraction, 3= acetone fraction, 4= methanol fraction. (A) 4 fractions compared to standards of oleic acid, MGDG (Monogalactosyldiacylglycerol), DGDG (Digalactosyldiacylglycerol), DOPG (1,2-Dioleoyl-*sn*-glycero-3-phospho-(1'-*rac*-glycerol)) and TG (triglycerides); (B) chloroform fraction compared to neutral lipid standards: MG, DG and TG (Mono-, Di- and Tri- glycerides) and FFA (free fatty acid).

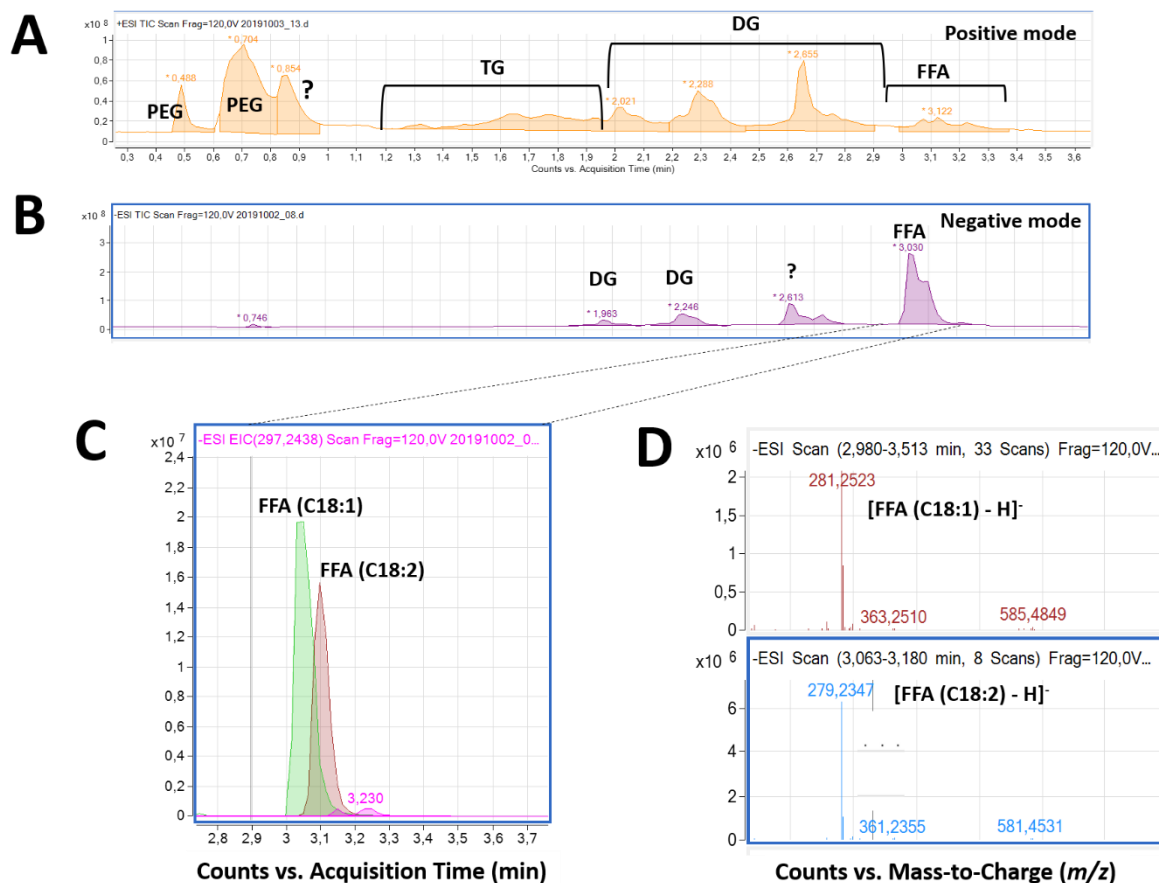


Figure S2: LC-MS analysis of the chloroform fraction of lipids of *C. maltaromaticum* CNCM I-3298 showing the presence of free fatty acids (FFA), triglycerides (TG) and diglycerides (DG). ESI total ion chromatogram in the positive (A) and in the negative (B) ion mode. (C) Zoom on the FFA peak. (D) MS signal of principal FFA in the negative ion mode. PEG (Polyethyleneglycol signal was attributed to contaminants).

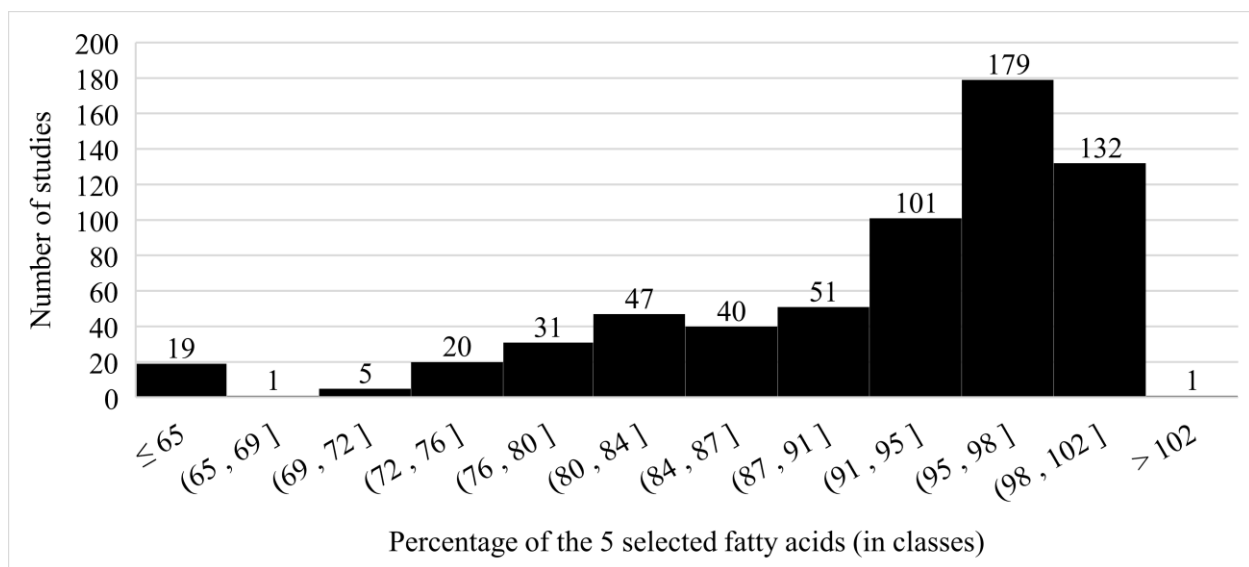


Figure S3: Number of studies corresponding to the sum of the proportion of the five fatty acids (C14:0, C16:0, C16:1, C18:1 and cycC19:0) ranged in class.

Table S1: Chemical shifts (ppm) observed in HSQC experiments of acetone fraction

Sugar	H1	H2	H3	H4	H5	H6a	H6b
	C1	C2	C3	C4	C5	C6	
α-Glc	5.00	3.59	3.56	3.43	3.77	3.76	
	96.70	76.60	72.00	69.90	71.90	61.40	
α-Gal	5.00	3.79	3.79	3.94	4.08	3.78	3.73
	96.70	69.10	70.20	69.70	71.00	61.80	

Table S2: Chemical shifts (ppm) observed in HSQC experiments for glycerol signals from acetone fraction

H1a	H1b	H2	H3a	H3b
C1		C2	C3	
4.44	4.19	5.23	3.84	3.65
62.7		69.95	65.90	